

First, a bit more about vision and eyes

Design Principles of Insect and Vertebrate Visual Systems

Joshua R. Sanes^{1,*} and S. Lawrence Zipursky^{2,*}

¹Center for Brain Science and Department of Molecular and Cellular Biology, Harvard University, Cambridge, MA 02138, USA

²Department of Biological Chemistry, Howard Hughes Medical Institute, David Geffen School of Medicine, University of California, Los Angeles, Los Angeles, CA 90095, USA

*Correspondence: sanesj@mcb.harvard.edu (J.R.S.), lzipursky@mednet.ucla.edu (S.L.Z.)

DOI 10.1016/j.neuron.2010.01.018

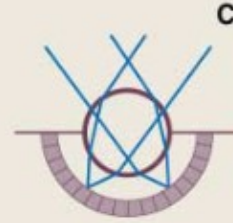
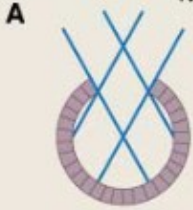
A century ago, Cajal noted striking similarities between the neural circuits that underlie vision in vertebrates and flies. Over the past few decades, structural and functional studies have provided strong support for Cajal's view. In parallel, genetic studies have revealed some common molecular mechanisms controlling development of vertebrate and fly visual systems and suggested that they share a common evolutionary origin. Here, we review these shared features, focusing on the first several layers—retina, optic tectum (superior colliculus), and lateral geniculate nucleus in vertebrates; and retina, lamina, and medulla in fly. We argue that vertebrate and fly visual circuits utilize common design principles and that taking advantage of this phylogenetic conservation will speed progress in elucidating both functional strategies and developmental mechanisms, as has already occurred in other areas of neurobiology ranging from electrical signaling and synaptic plasticity to neurogenesis and axon guidance.

Evolutionists
thought eyes
evolved many
times
independently

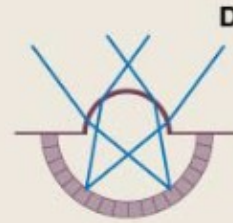
Chambered eyes



Nautilus



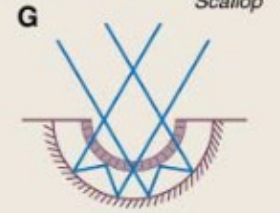
Octopus



Red-tailed hawk



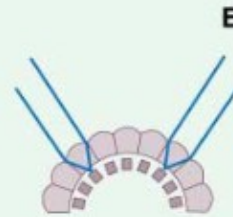
Scallop



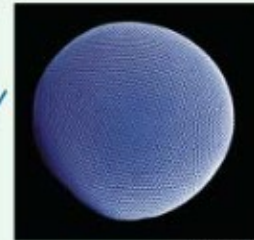
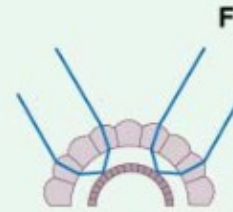
Compound eyes



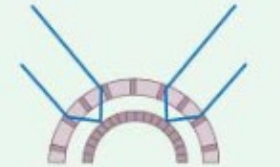
Sea fan



Dragonfly

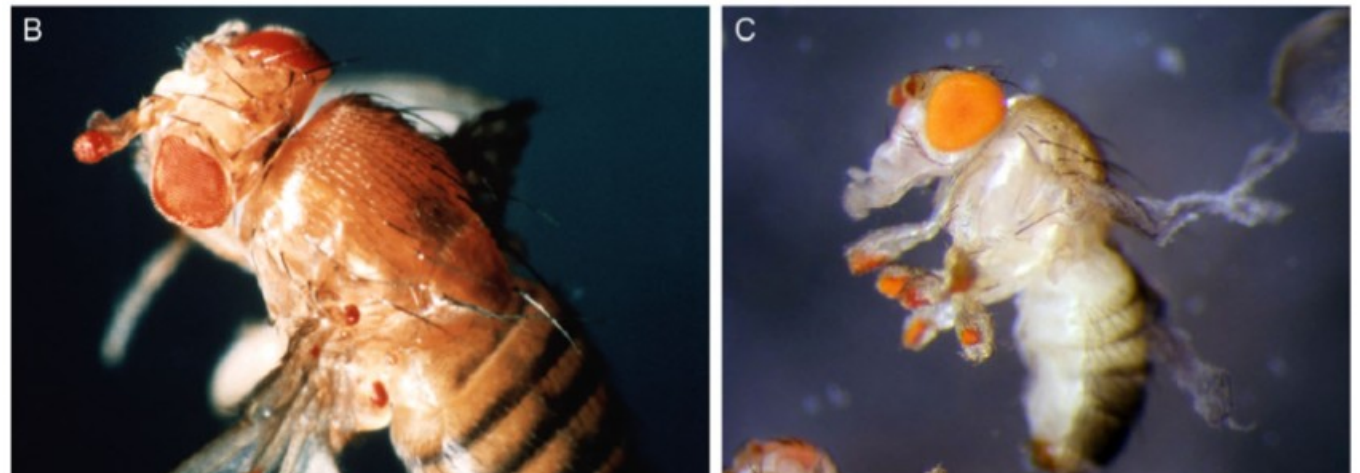
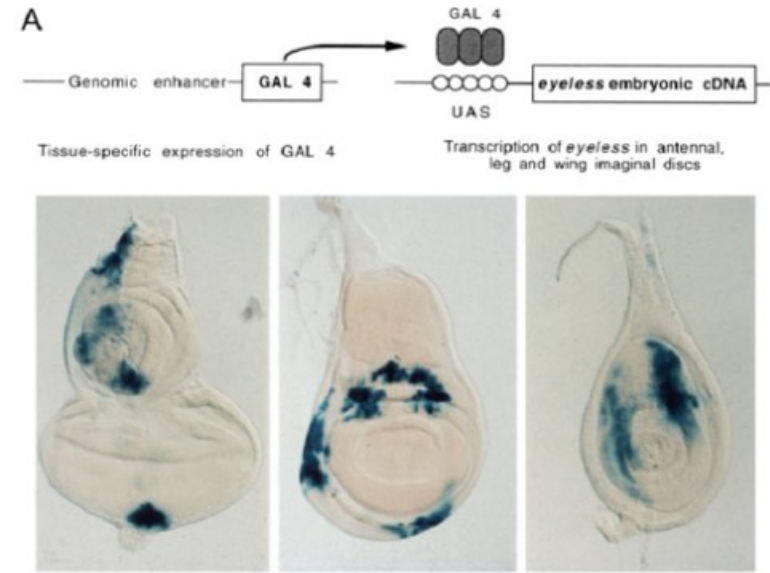


Krill eye



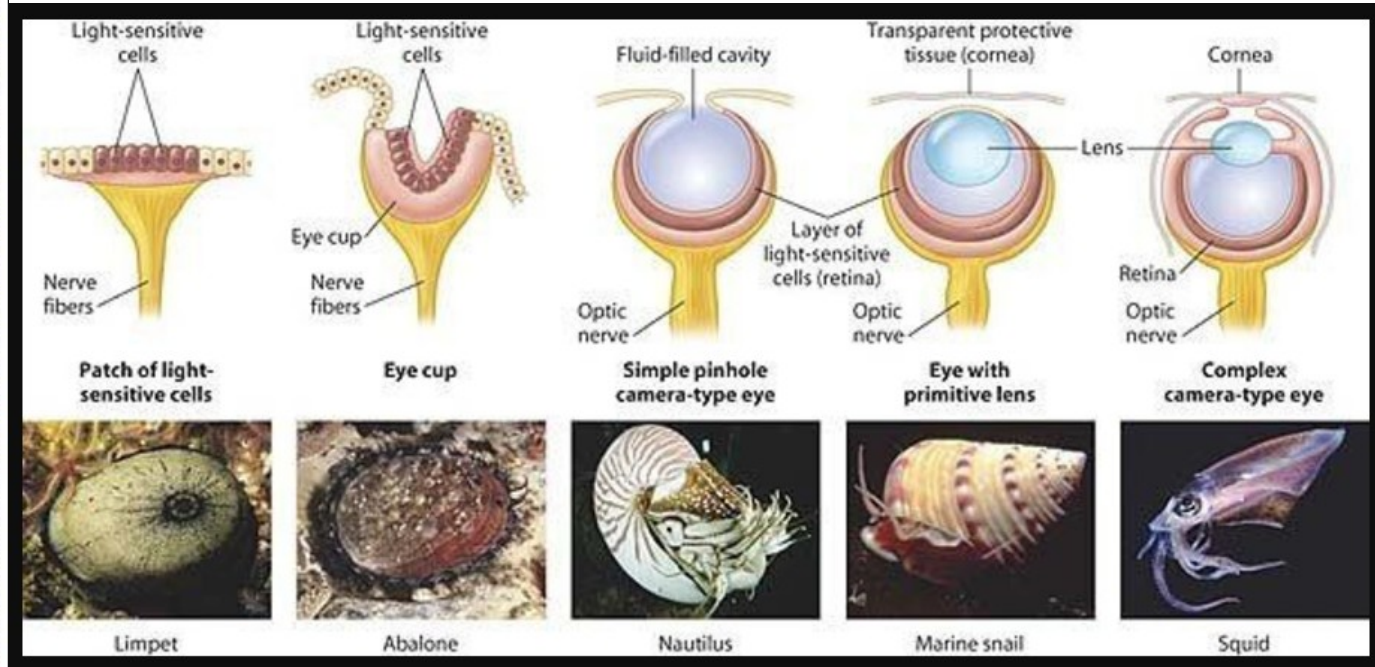
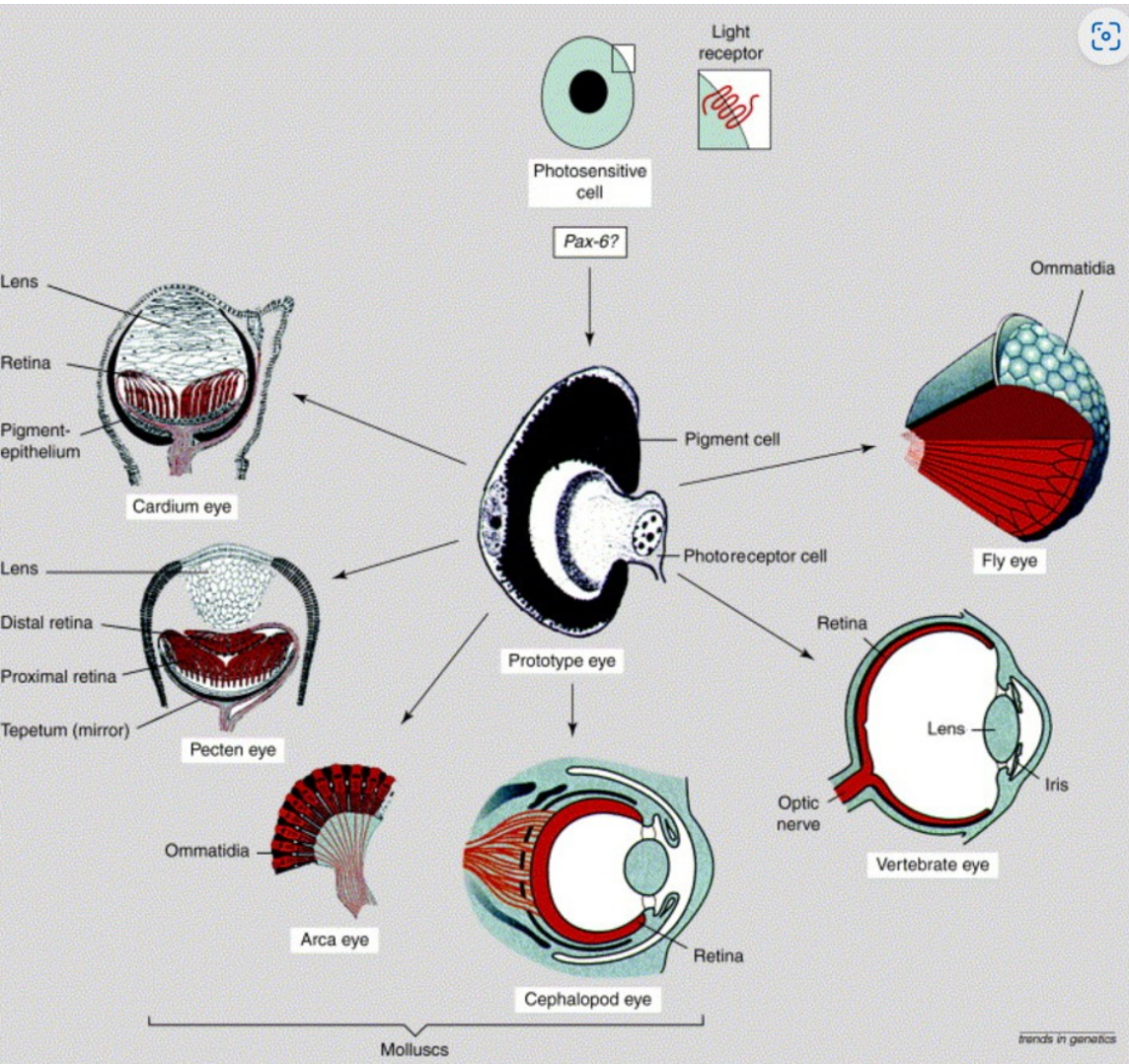
Lobster

However, discovery of *Eyeless/PAX6* suggests eyes are all evolutionarily related



—Targeted expression of *eyeless* (*ey*) and induction of ectopic eyes in *Drosophila* (after Halder et al. 1995). (A) Targeted expression of *ey* cDNA using a genomic enhancer to induce the yeast *gal4* transcription factor driving *ey* cDNA in various imaginal discs. Gal4 binds to its upstream activating sequences (UASs) and drives the expression of *ey* into the respective areas of the eye-antenna, wing, and leg discs (blue). (B) Ectopic induction of eyes on the antenna and mesothorax. (C) Ectopic induction of eyes on all six legs by using the decapentaplegic enhancer.

Eyeless/PAX6 suggests eyes are all evolutionarily related



Ramon y Cajal saw that insect and vertebrate eyes have similar neuron types

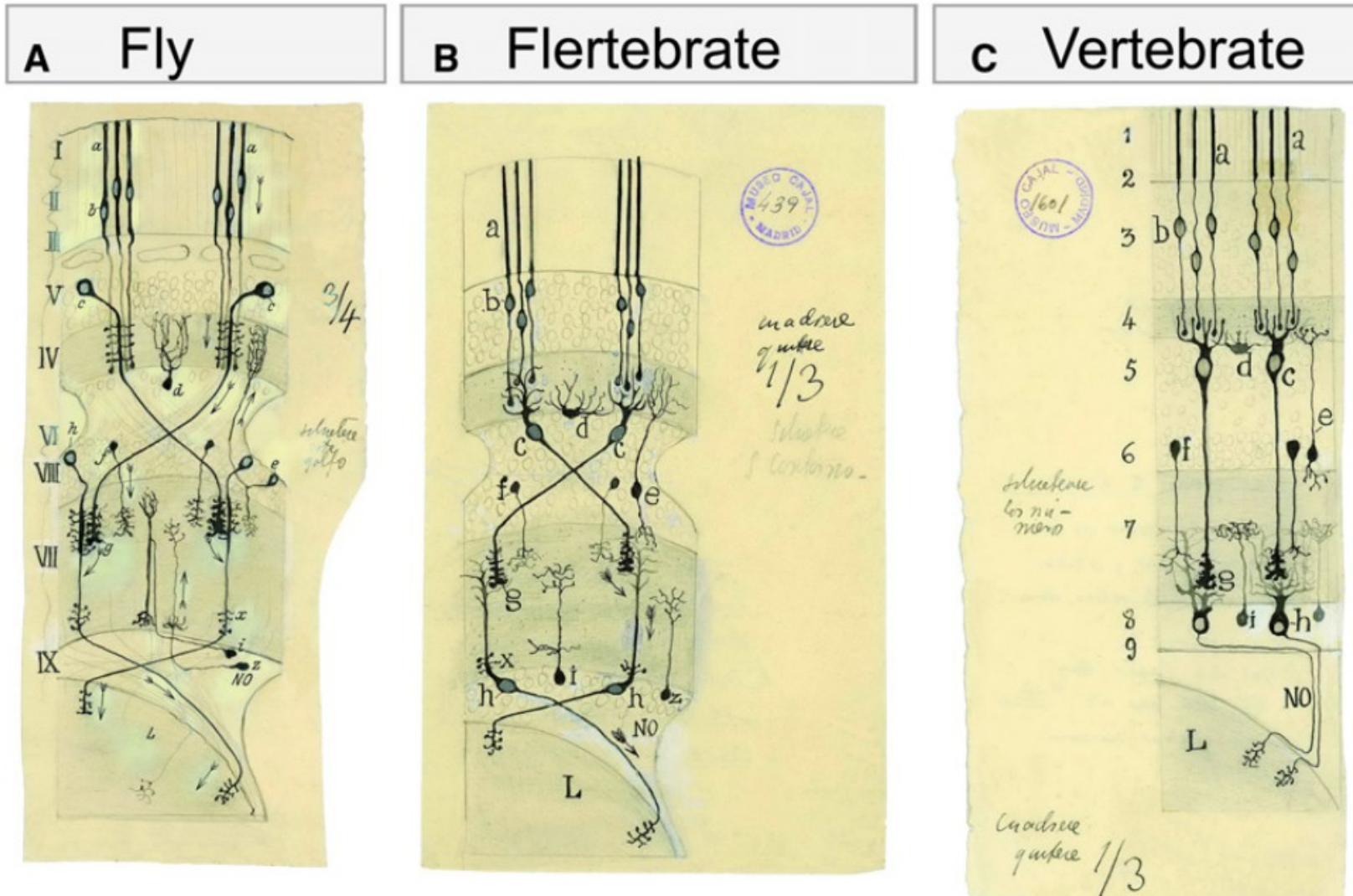


Figure 3. Cajal Recognized the Similarity of Fly and Vertebrate Visual Systems

(A) The retina (I – III), lamina (IV and V), and medulla (VI and VIII) and lobula region (L) of the fly visual system. The somas appear in their natural position. a and b, photoreceptor; c, lamina monopolar neuron; h, transmedullary neuron.

(B) In this drawing of the insect visual system, Cajal “moved” the cell bodies to correspond to their positions in vertebrates, without changing the positions of their synaptic contacts. We refer to this as the “Flertebrate” arrangement. c, lamina monopolar neurons take on the appearance of bipolar neurons (see “c” in right panel); d, amacrine cells in the fly appear as horizontal cells (see “d” in right panel). h, transmedullary cells appear as retinal ganglion cells (see “h” in right panel).

(C) Schematic of the main cell types in the vertebrate retina and their connections. The Arabic numerals indicate regions of the vertebrate retina that Cajal viewed as similar to the corresponding layers marked with Roman numerals in the left panel. From Cajal and Sanchez, 1915; adapted from Meinertzhagen, 1993.

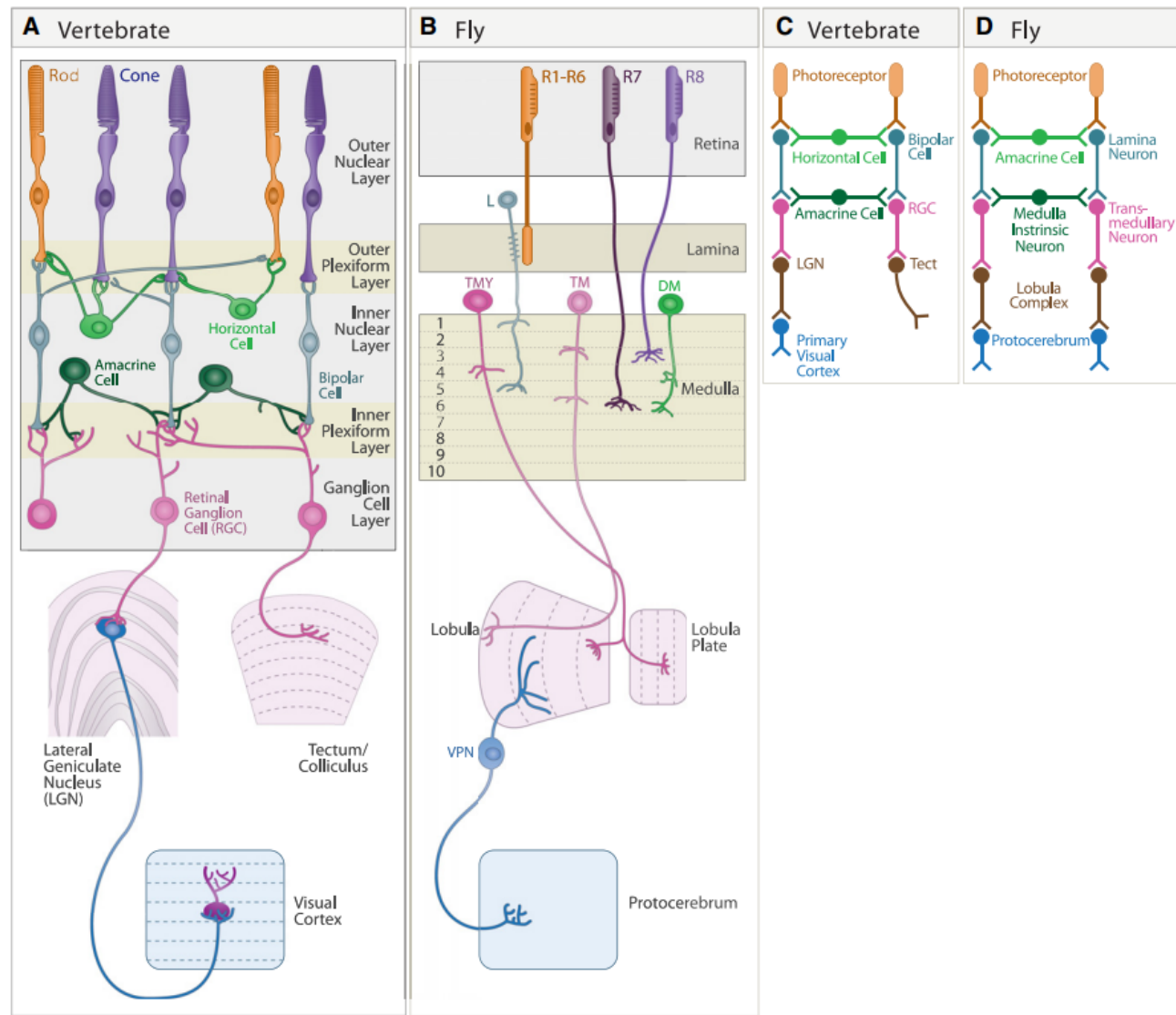


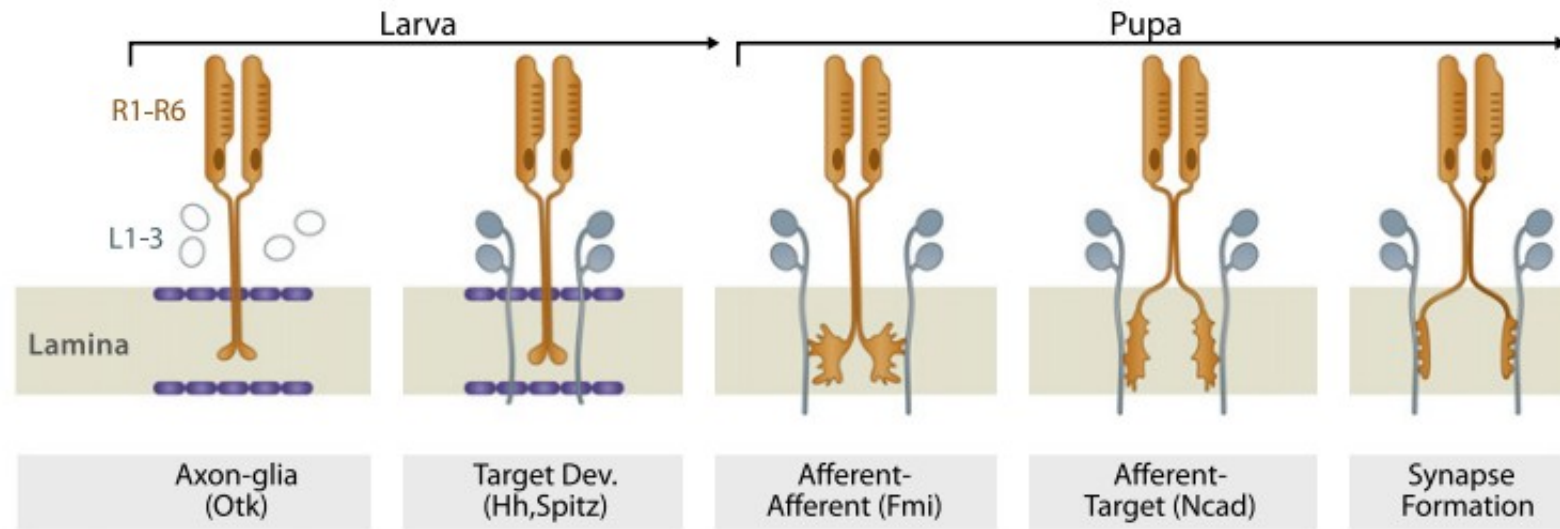
Figure 1. Structures Underlying the First Stages of Visual Processing

(A) Mammalian visual system, showing retina, dorsal lateral geniculate nucleus (LGN), superior colliculus (called optic tectum in lower vertebrates), and primary visual cortex (also called Area 17, striate cortex, or V1). Main retinal cell types are indicated.

(B) *Drosophila* visual system, showing retina, lamina, medulla, and the lobula complex, which comprises the lobula and lobula plate. A few cell types are shown.

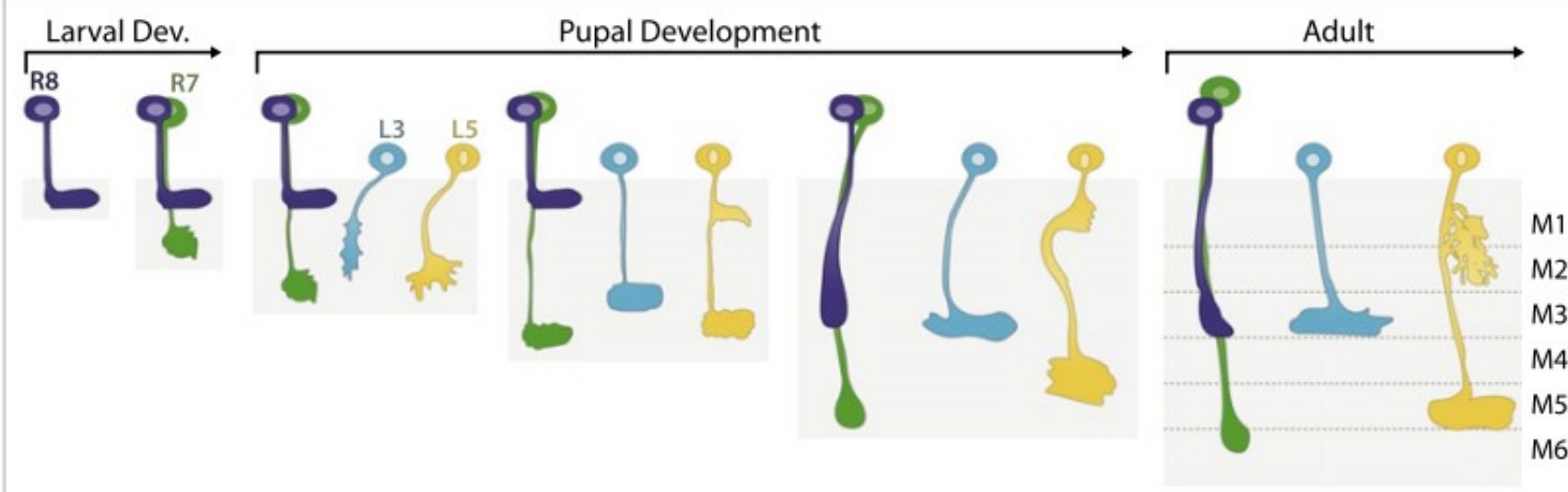
(C and D) Similar steps in transfer of information through early stages of vertebrate and *Drosophila* visual systems.

C Fly Lamina



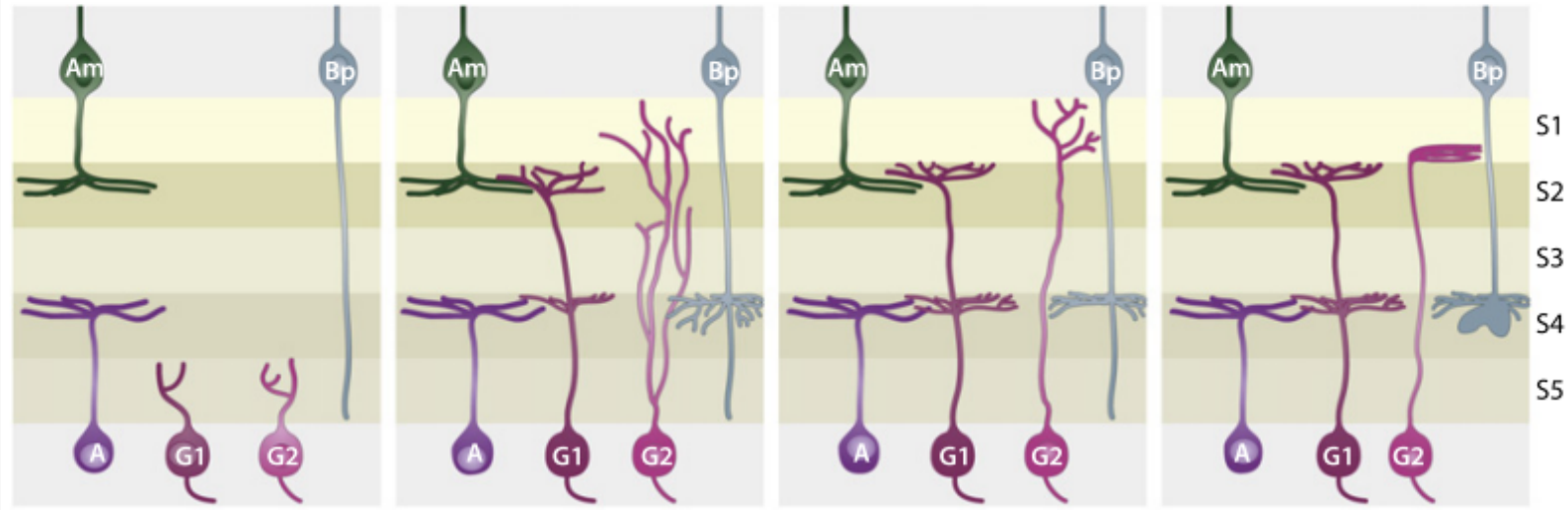
(C) Fly lamina. The growth cones of R1–R6 axons from the same ommatidium initially terminate in a tight cluster in a temporary layer bounded by glia. Interactions between growth cones promote extension away from one another in defined orientations where each projects to a different set of lamina neurons in surrounding cartridges and forms synapses with them. Some of the molecules implicated in discrete steps are indicated.

D Fly Medulla



(D) Fly medulla. The axons of R7, R8, L3, and L5 exhibit cell-type-specific behaviors as they form lamina-specific terminals in the medulla.

A Vertebrate Inner Plexiform Layer (IPL)



B Vertebrate Lateral Geniculate Nucleus (LGN)

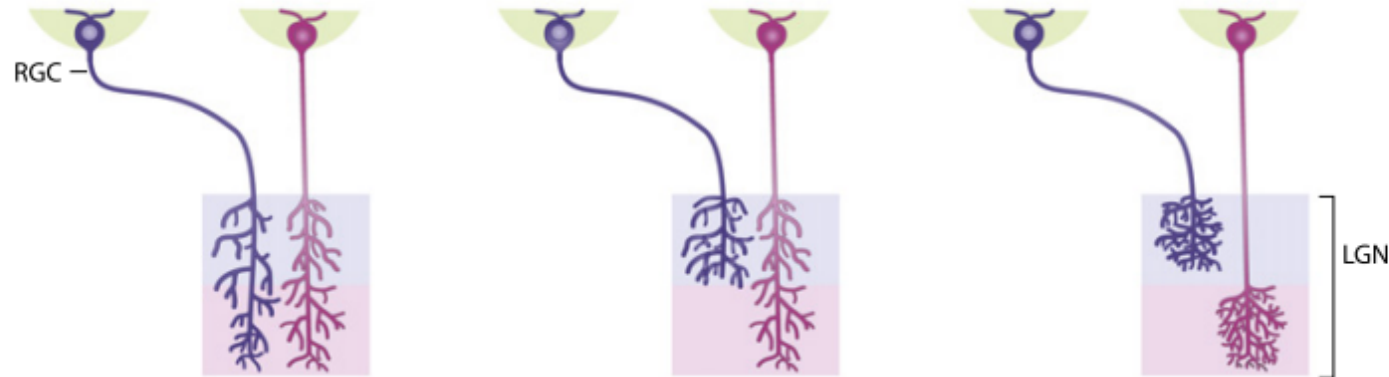


Figure 10. Formation of Lamina-Specific Connections

(A) Inner plexiform layer. Processes of many amacrine cells ramify from the outset in appropriate sublaminae. Development of RGC dendrites exhibits subtype-specific variations: arbors of some types are initially diffuse then remodel, others are lamina-restricted from an early stage, and still others develop in discrete steps. The first two are shown here. Bipolar cells are born and extend axons late; their processes initially span multiple sublaminae, then become lamina-restricted. The IPL expands and sublaminae form as processes enter it and arborize. For clarity, we do not show this thickening here.

(B) Lateral geniculate nucleus. Axons from the ipsi- and contralateral eyes initially arborize broadly. Activity-dependent processes promote refinement to appropriate target laminae.

(C) Fly lamina. The growth cones of R1–R6 axons from the same ommatidium initially terminate in a tight cluster in a temporary layer bounded by glia. Interactions between growth cones promote extension away from one another in defined orientations where each projects to a different set of lamina neurons in surrounding cartridges and forms synapses with them. Some of the molecules

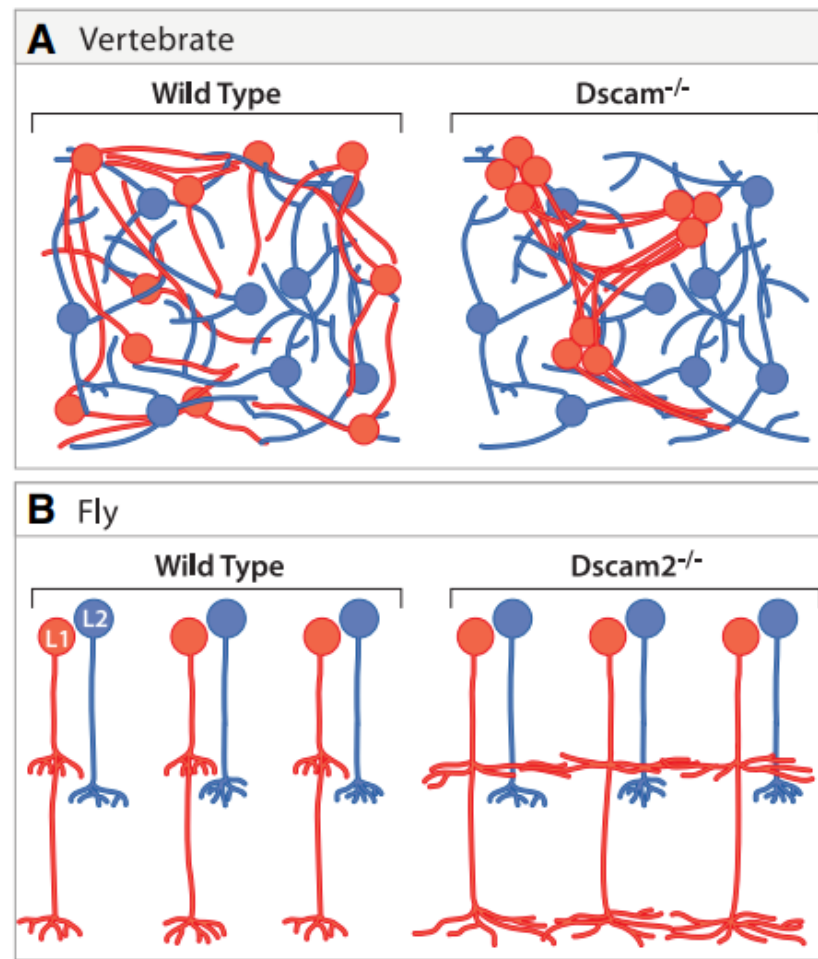
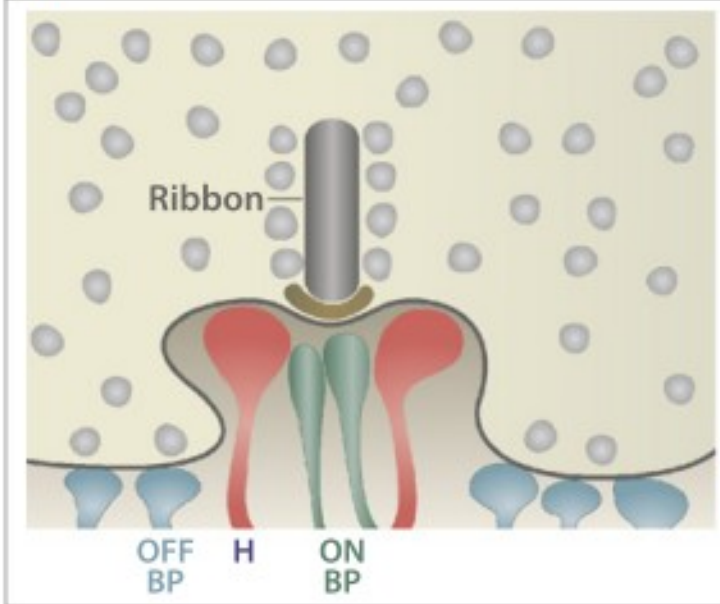


Figure 9. Dscam Proteins Mediate Homotypic Repellent Interactions Required for Tiling of Visual Interneurons

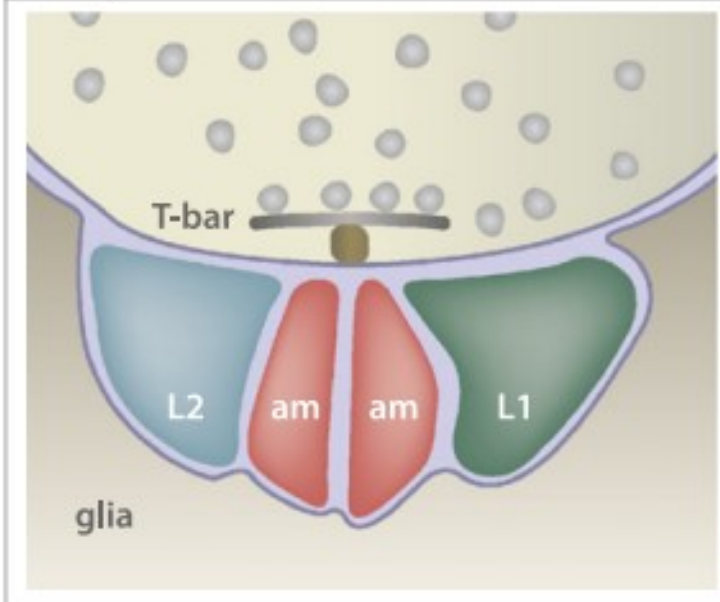
(A) Dscam is expressed in several amacrine cell subsets in mouse retina. In mutants lacking Dscam, processes of these cells fasciculate and, in consequence, their mosaic arrangement is later perturbed. Other amacrine subtypes, which did not express Dscam, are unaffected.

(B) Dscam2 is required selectively in L1 neurons for tiling in the medulla. Terminals of L1 neurons lacking Dscam2 extend into neighboring cartridges. Tiling of L2 axon terminals is normal in Dscam2 mutants.

A Vertebrate



B Fly

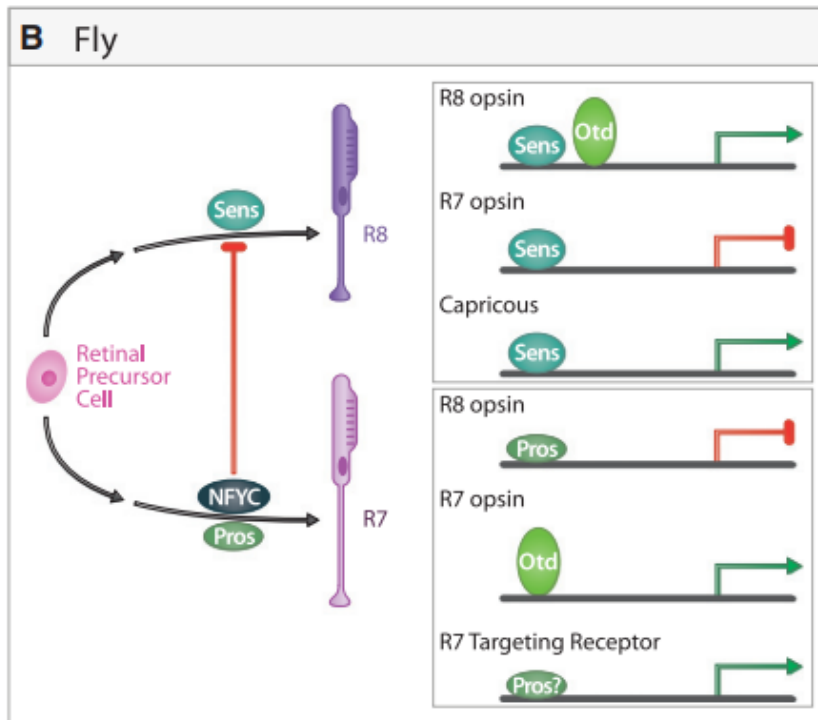
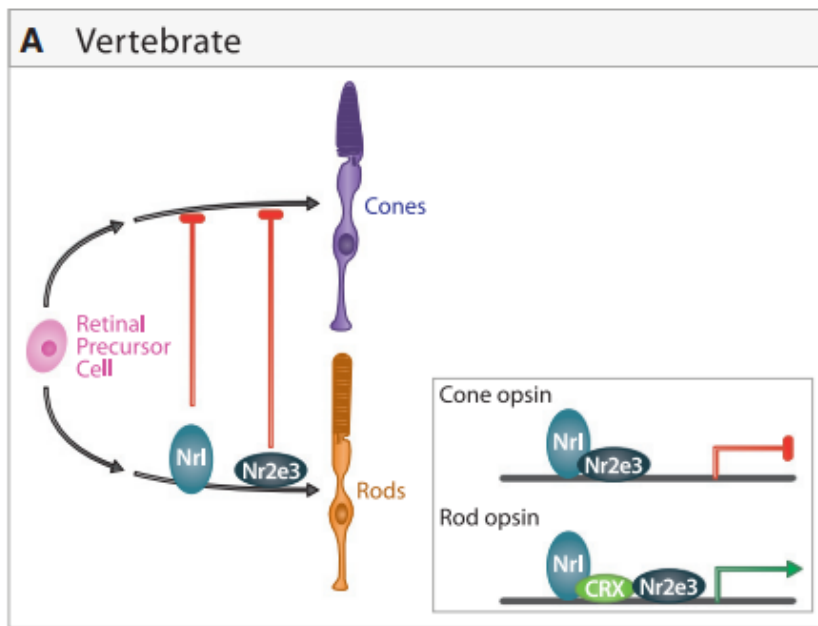


Vertebrate and fly first visual synapses are both large and multiple contact

Figure 4. Multiple Contact Synapses

(A) Portion on a cone pedicle in the outer plexiform layer, showing its synapses with processes of multiple horizontal, ON bipolar, and OFF bipolar cells. The ribbon structure at the active zone of these synapses is specialized for tonic transmitter release. Multiple contact synapses are also common in the IPL.

(B) Tetrad in *Drosophila* lamina, showing synapses of photoreceptor axon on processes of L1, L2, and amacrine (am) cell dendrites. Like the vertebrate photoreceptor, that of *Drosophila* contains an unusually large presynaptic specialization, in this case a T bar (T). Schematic is simplified to show all post-synaptic elements in the same plane; L1 and L2 are paired equatorially, while the am elements are paired in polar positions. In some cases, one amacrine cell process is replaced with a process from L3. Multiple contact synapses are the predominant type of synapse throughout the fly central nervous system.



Some transcriptional regulators of eye cell types and *opsin* genes are conserved

Figure 8. Transcriptional Control of Photoreceptor Diversification

(A) Regulation of photoreceptor subtype identity in the mouse retina. *Nrl* and *Nr2e3* promote rod development and repress cone cell programs in rods. These transcription factors also regulate photoreceptor-subtype-specific expression of opsins in rods and are likely to regulate other genes controlling rod and cone cell development (adapted from Onishi et al., 2009).

(B) Regulation of photoreceptor subtype in fly retina. NF-YC represses a part of the R8 developmental program in R7 by preventing *Senseless* expression. *Senseless* regulates R8 and R7 subtype-specific opsin expression in R8 and has also been implicated in expression of *Capricious* and other genes regulating R8 targeting. *Prospero* also regulates opsin expression and acts in parallel with other transcription factors to regulate R7 targeting. R7 and R8 subtypes can be further divided by the opsins they express (see text). *Otd* and *Crx* are homologous and play key roles in regulating opsin expression in both flies and mice.

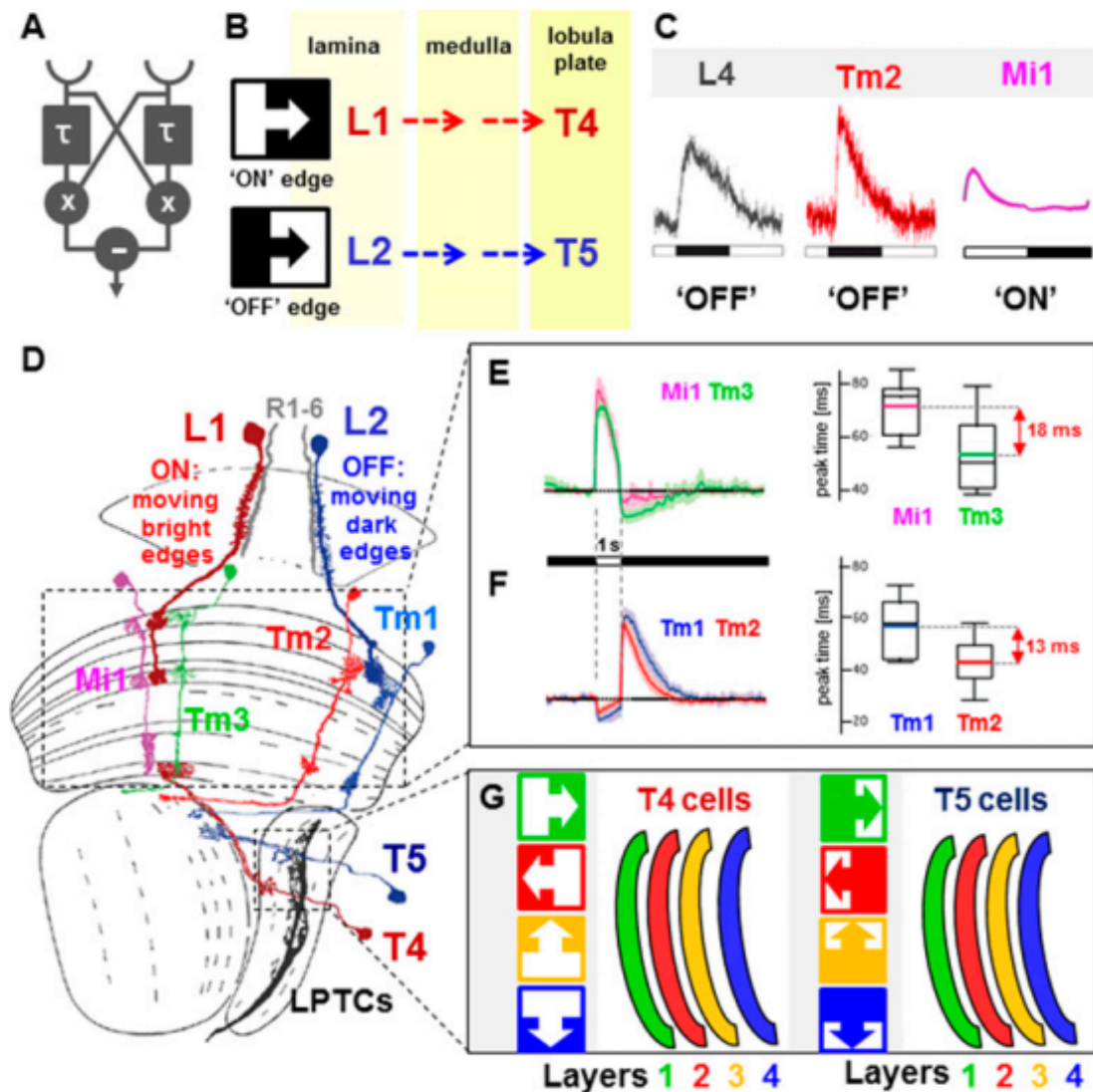


Figure 6. Functional characterization of *Drosophila* optic lobe neurons. (A) Summary of the computational model for EMDs receiving input from two points in space (semicircles) first proposed by Hassenstein and Reichardt (1956). (τ) Time constant of a delay channel; (\times) multiplication; ($-$) subtraction. (Adapted from Borst and Euler 2011 with permission from Elsevier). (B) Based on previous work, moving light edges (ON) and dark edges (OFF) are detected by lamina monopolar cells L1 and L2, respectively. The information is then transmitted to the lobula plate, where T4 and T5 cells relay ON and OFF signals onto direction-selective output cells. (C) Characterization of two cell types in the lamina (L4) and medulla neuropil (Tm2) using genetically encoded calcium sensor GCaMP5 and two-photon microscopy. Both cell types are activated specifically by OFF edges, thereby placing them in the OFF pathway between L2 and T5 (adapted from Meier et al. 2014 with permission from Elsevier; adapted from Strother et al. 2014 with permission from Elsevier). (D) Based on large-scale anatomical reconstruction of optic lobe tissue using serial EM reconstruction, the cellular substrates for the ON/OFF pathways leading from the retina to the movement-sensitive LPTCs were proposed. One arm of the pathway is specialized for moving bright edges (R1-6 \rightarrow L1 \rightarrow Mi1/Tm3 \rightarrow T4), and the other one is specialized for moving dark edges (R1-6 \rightarrow L2 \rightarrow Tm1/Tm2 \rightarrow T5). (E) Electrophysiological characterization of the Mi1/Tm3 ON arm of the elementary motion

detector. Both cells are hyperpolarized by light increments, and a significant time delay (18 msec) exists between the two cell types (adapted from Behnia et al. 2014). (F) In contrast, Tm1/Tm2 cells of the OFF arm are activated by light decrements and also manifest a significant delay (13 msec) (adapted from Behnia et al. 2014). (G) Functional characterization of direction-selective cells in the lobula plate using calcium imaging. Dendrites of T4 cells are excited maximally by moving bright edges, while T5 dendrites respond to moving dark edges. Dendrites responding to different cardinal directions locate to different layers. (Green) right; (red) left; (yellow) up; (blue) down. (Adapted by permission from Macmillan Publishers Ltd. from Maisak et al. 2013).

Lecture 9. Olfaction, learning and memory. 22.11.24

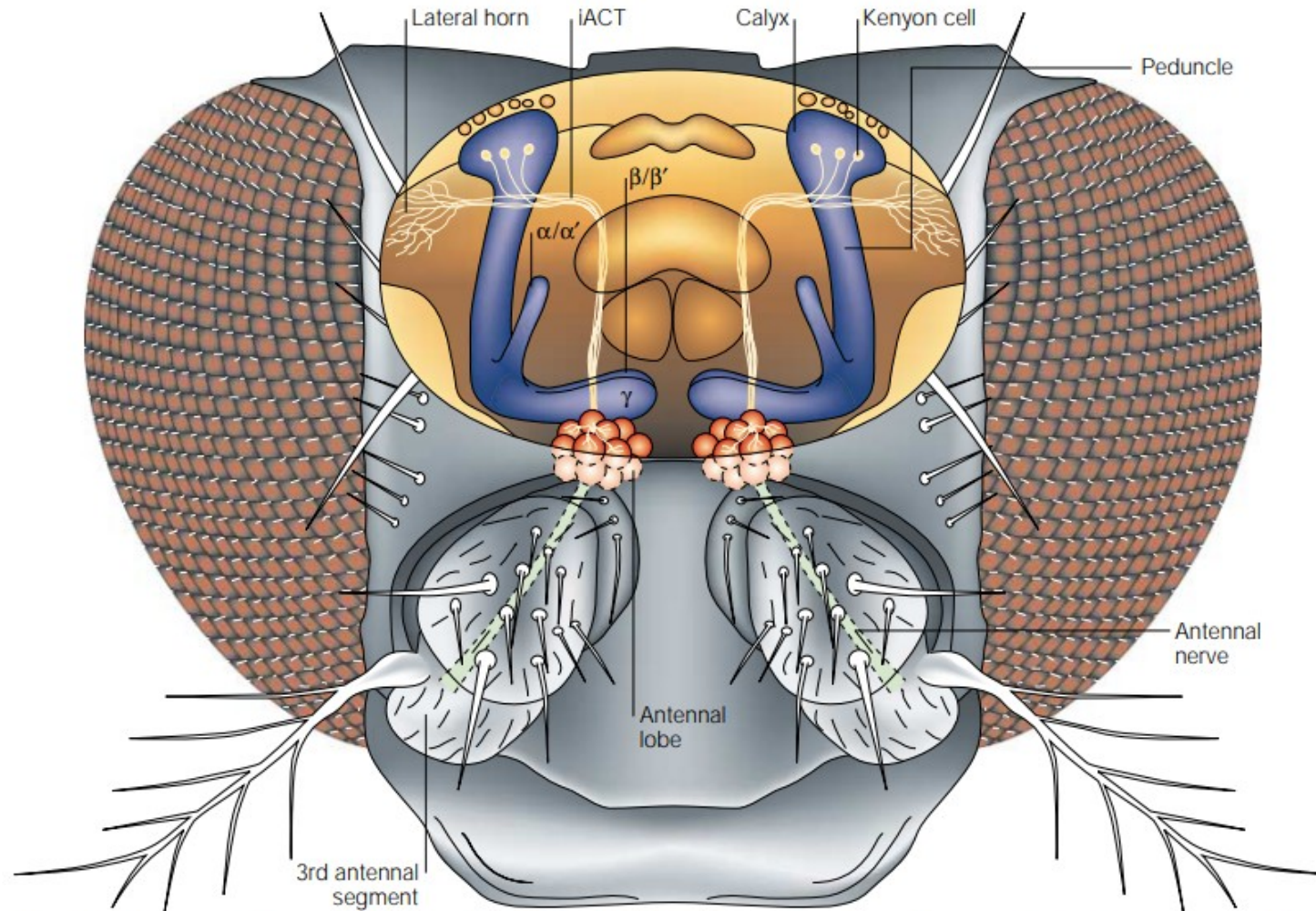


Figure 2 | **Olfactory pathway.** Odour information is carried from the third antennal segments and maxillary palps (not shown) to the antennal lobe, where receptor fibres are sorted according to their chemospecificities in about 40 glomeruli. These represent the primary odour qualities, which are reported to two major target areas in the brain, the dorsolateral protocerebrum (lateral horn) and the calyx of the mushroom body. The inner antennocerebral tract (iACT) connects individual glomeruli to both areas. α/α' , β/β' and γ mark the three mushroom body subsystems described by Crittenden *et al.* (REF. 64).

Leading Edge

Review

Cell

Olfactory Perception: Receptors, Cells, and Circuits

Chih-Ying Su,^{1,2} Karen Menuz,^{1,2} and John R. Carlson^{1,*}

¹Department of Molecular, Cellular, and Developmental Biology, Yale University, New Haven, CT 06520, USA

²These authors contributed equally to this work.

*Correspondence: john.carlson@yale.edu

DOI 10.1016/j.cell.2009.09.015

Remarkable advances in our understanding of olfactory perception have been made in recent years, including the discovery of new mechanisms of olfactory signaling and new principles of olfactory processing. Here, we discuss the insight that has been gained into the receptors, cells, and circuits that underlie the sense of smell.

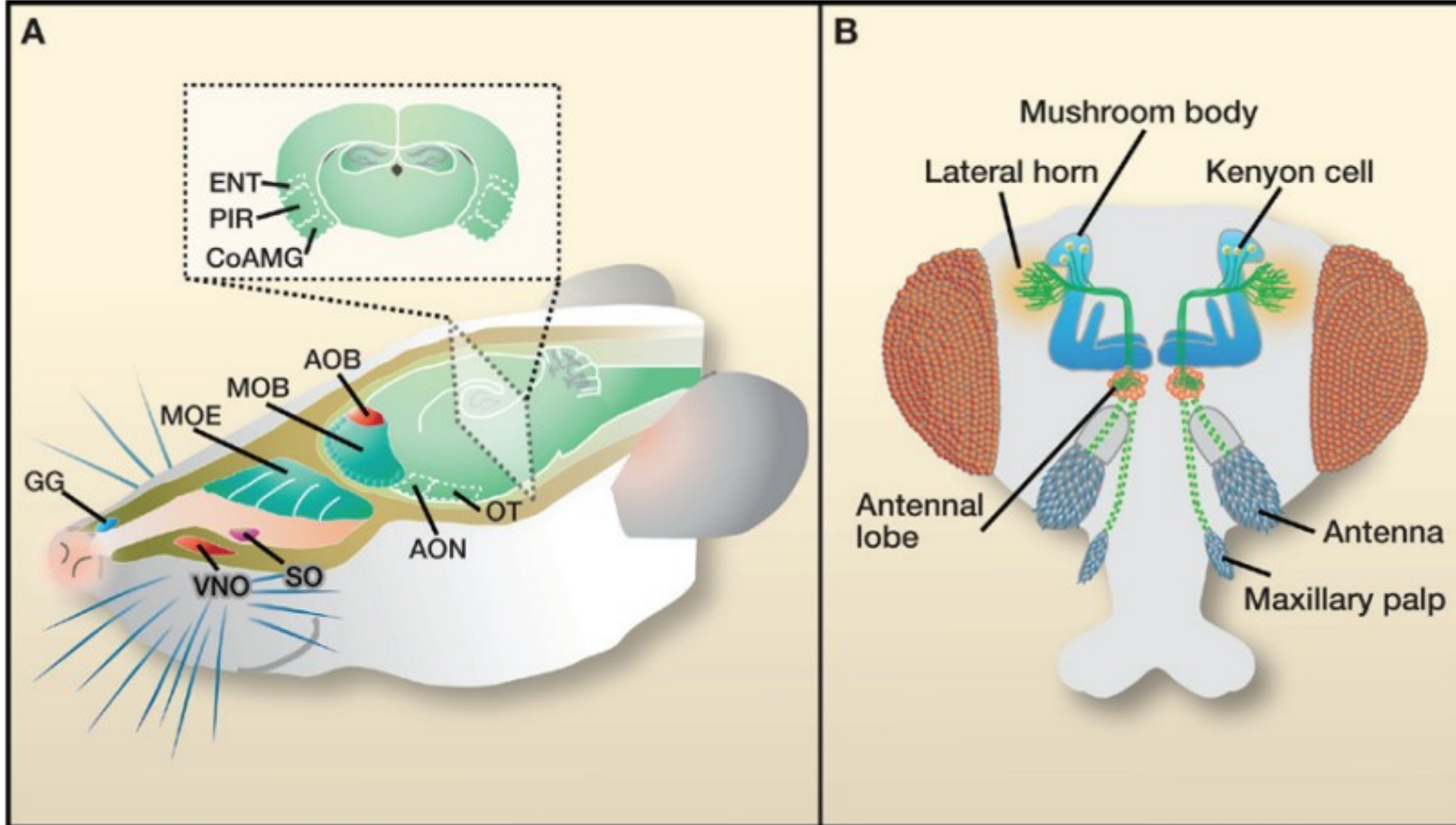


Figure 1. Olfactory System Anatomy

(A) Sagittal view of a rodent head, showing four olfactory organs: the main olfactory epithelium (MOE), vomeronasal organ (VNO), Grueneberg ganglion (GG), and septal organ of Masera (SO). Olfactory receptor neurons (ORNs) in the MOE, GG, and SO all project to the main olfactory bulb (MOB), whereas the VNO neurons project to the accessory olfactory bulb (AOB). Olfactory information is further processed in higher brain regions, such as the anterior olfactory nucleus (AON), the olfactory tubercle (OT), entorhinal cortex (ENT), piriform cortex (PIR), and cortical amygdala (CoAMG). Inset: coronal section of the brain.

(B) Frontal view of a *Drosophila* head. There are two pairs of olfactory organs: the third antennal segments and maxillary palps. Olfactory information is first relayed to the antennal lobe, which contains multiple glomeruli. Subsequent processing takes place at the lateral horn of the protocerebrum and Kenyon cells in the mushroom body. Connectivity has been simplified for clarity.

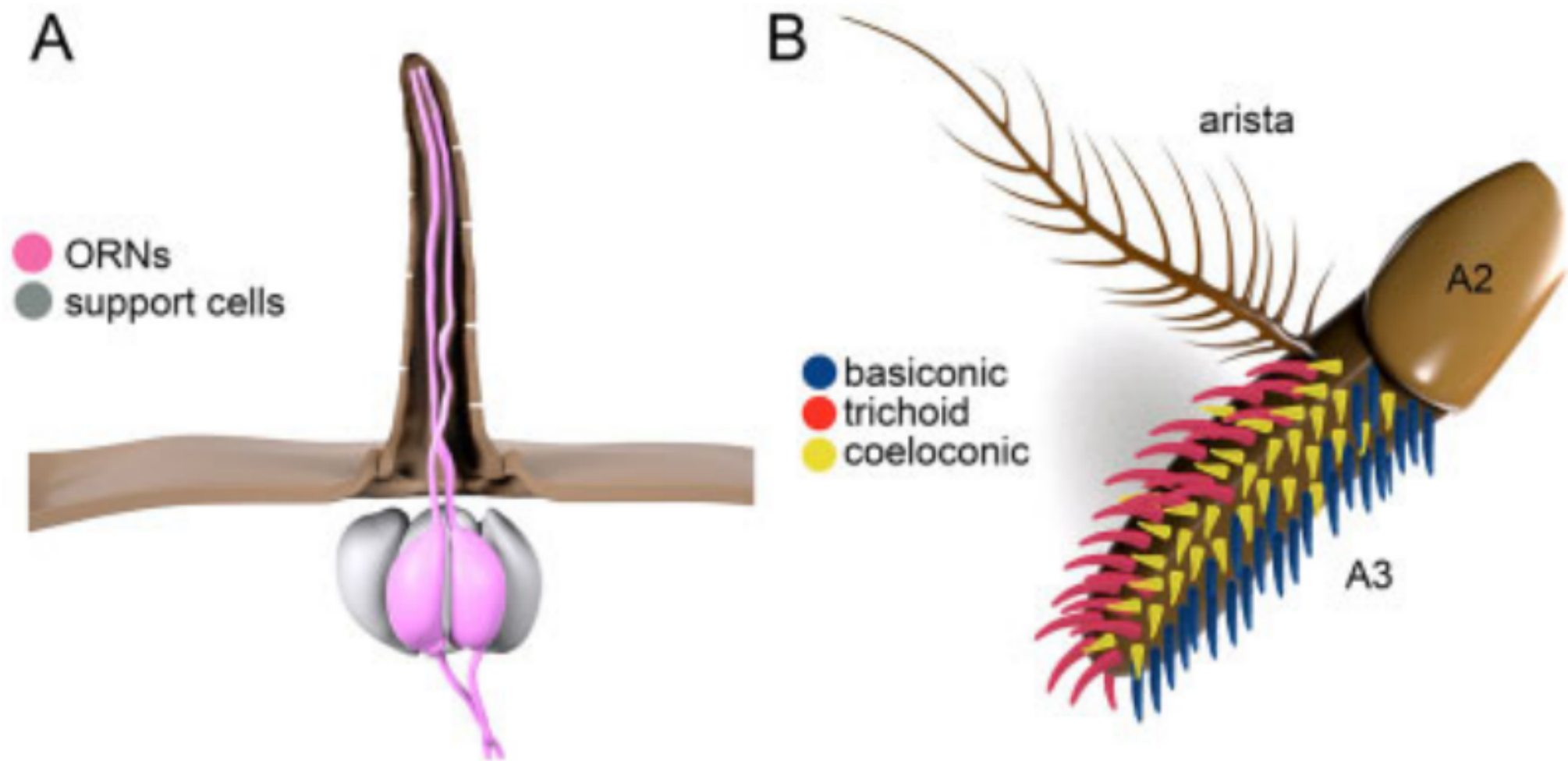


Figure 6. Olfactory sensilla. (A) Olfactory sensilla housing two neurons. The support cells and the distribution of pores are also indicated. (B) Antenna. The distributions of three types of olfactory sensilla are indicated. A2, second antennal segment; A3, third antennal segment.

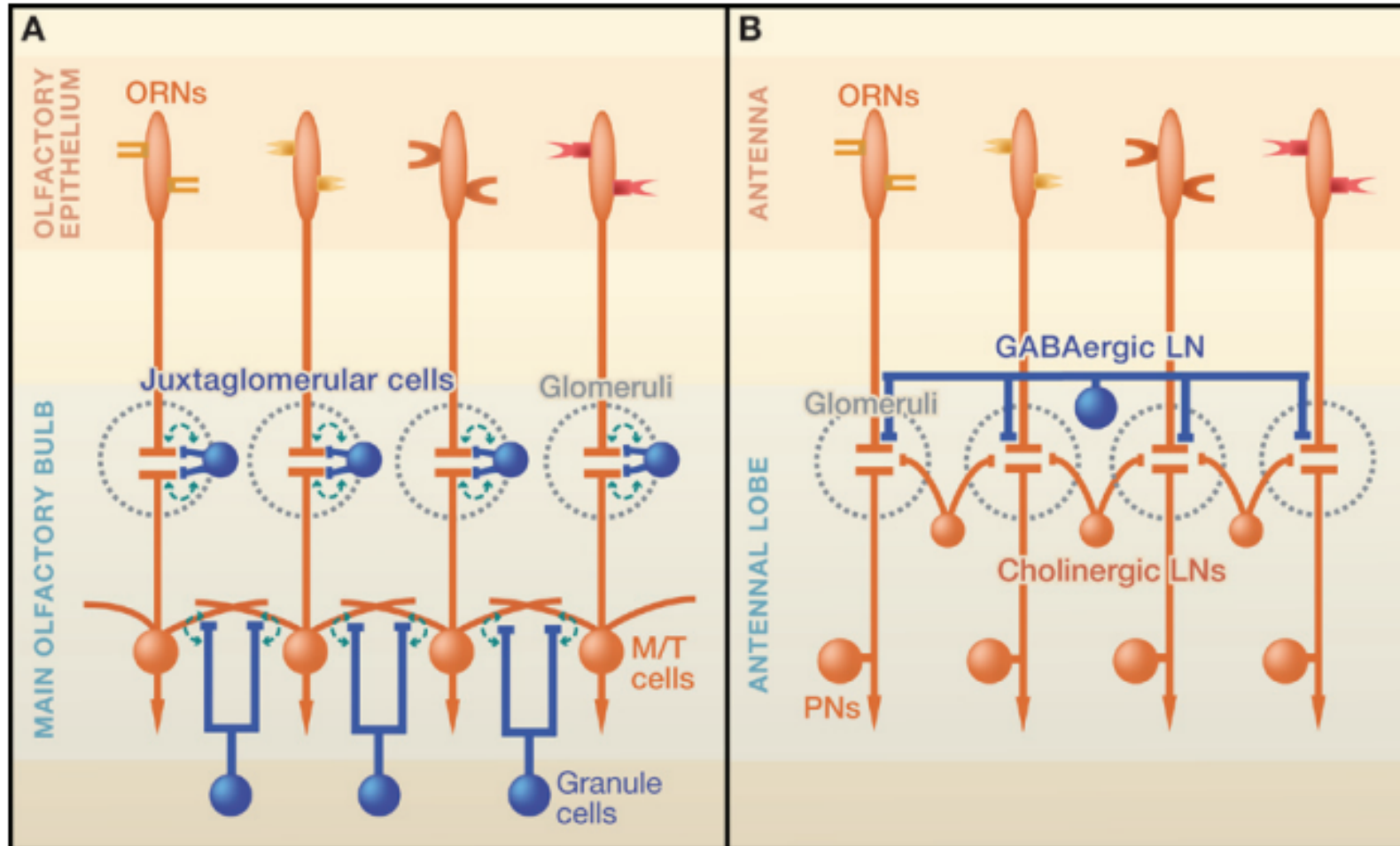


Figure 2. Olfactory Bulb and Antennal Lobe Circuitry

Excitatory neurons are shown in orange and inhibitory neurons in blue.

(A) Olfactory receptor neurons (ORNs) in the olfactory epithelium that express different olfactory receptors project axons to separate glomeruli (dashed outlines) in the olfactory bulb where they synapse on mitral and tufted (M/T) cells, whose apical dendrite is usually localized to a single glomerulus. Juxtglomerular cells (blue) contribute to intraglomerular inhibition. In the glomerulus, ORNs form synapses on juxtglomerular cell dendrites, which in turn inhibit ORN axon terminals. Reciprocal synapses are also found between juxtglomerular cell and M/T cell dendrites. Reciprocal synapses are formed between the dendrites of granule cells and M/T cells. M/T cells excite granule cells, which respond by inhibiting M/T cells. Due to the lateral spread of M/T secondary dendrites, granule cells contact multiple M/T cells associated with different glomeruli, and thus can mediate both intra- and interglomerular inhibition.

(B) In *Drosophila*, ORNs expressing the same olfactory receptors in the antenna or maxillary palp synapse on projection neurons in a single glomerulus, analogous to the olfactory bulb. GABA-releasing local neurons (LNs) presynaptically inhibit ORN axon terminals in multiple glomeruli, mediating interglomerular inhibition. Excitatory cholinergic LNs mediate interglomerular excitation.

The Molecular Basis of Odor Coding in the *Drosophila* Antenna

Elissa A. Hallem, Michael G. Ho,
and John R. Carlson*
Department of Molecular, Cellular,
and Developmental Biology
Yale University
New Haven, Connecticut 06520

Summary

We have undertaken a functional analysis of the odorant receptor repertoire in the *Drosophila* antenna. Each receptor was expressed in a mutant olfactory receptor neuron (ORN) used as a “decoder,” and the odor response spectrum conferred by the receptor was determined in vivo by electrophysiological recordings. The spectra of these receptors were then matched to those of defined ORNs to establish a receptor-to-neuron map. In addition to the odor response spectrum, the receptors dictate the signaling mode, i.e., excitation or inhibition, and the response dynamics of the neuron. An individual receptor can mediate both excitatory and inhibitory responses to different odorants in the same cell, suggesting a model of odorant receptor transduction. Receptors vary widely in their breadth of tuning, and odorants vary widely in the number of receptors they activate. Together, these properties provide a molecular basis for odor coding by the receptor repertoire of an olfactory organ.

spheroidal modules, called glomeruli, in the brain (Resler et al., 1994; Vassar et al., 1994; Mombaerts et al., 1996; Gao et al., 2000; Vosshall et al., 2000). While there have been a number of descriptive studies of odorant receptor gene expression, there have been few functional studies of the receptors, either individually or collectively. The first odorant receptor to be functionally characterized was the *C. elegans* receptor *odr-10*, for which diacetyl was identified as a ligand (Sengupta et al., 1996). Odor response spectra of only a limited number of receptors have been characterized subsequently, in large part because expression in heterologous systems has proved difficult.

The fruit fly *Drosophila melanogaster* has two olfactory organs, the antenna and maxillary palp, which contain ~1200 and ~120 ORNs, respectively (Stocker, 1994; Shanbhag et al., 1999). ORNs are compartmentalized into sensilla, which can be subdivided into three major morphological types: basiconic, coeloconic, and trichoid. Each sensillum contains the dendrites of up to four ORNs.

Drosophila ORNs can be subdivided into distinct functional classes on the basis of their odor response spectra. Extensive electrophysiological characterization of the antennal basiconic sensilla identified 18 functional classes of ORNs, which are found in stereotyped combinations within eight types of sensilla (de Bruyne et al., 2001; Elmore et al., 2003). These ORNs show diverse responses to odorants: not only do they exhibit distinct odor response spectra but they can show excitatory or inhibitory responses, and they show different response

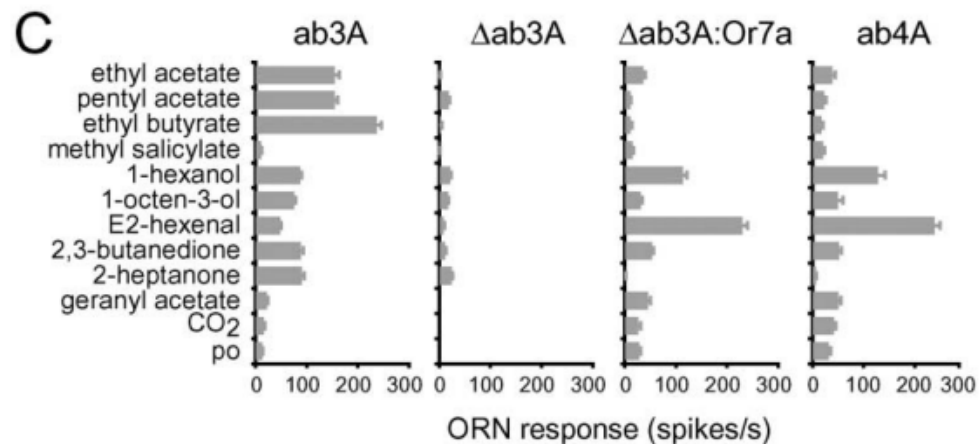
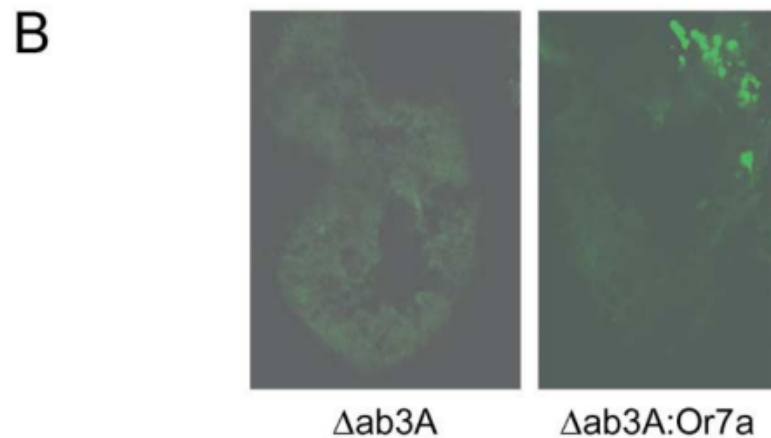
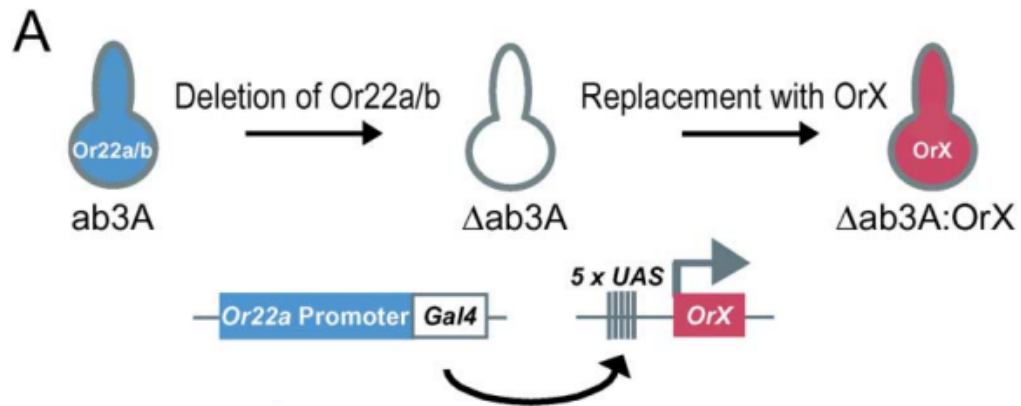


Figure 1. Analysis of Odor Response Spectra of Individual Odorant Receptors

(A) A mutant *ab3A* antennal neuron ($\Delta ab3A$) lacks odor response due to the deletion of its endogenous receptor genes, *Or22a* and *Or22b*. Odorant receptors are introduced specifically into $\Delta ab3A$ using the *GAL4/UAS* system. *Or22a-GAL4* is used to drive expression from a *UAS-Or* construct. The odorant response of the neuron ($\Delta ab3A:OrX$) is assayed electrophysiologically.

(B) Expression of *Or7a* in $\Delta ab3A$. Fluorescent immunolabeling of antennal sections with an anti-myc antibody labels a subset of dorsomedial sensilla where *ab3A* dendrites are located. The antenna on the left contains $\Delta ab3A$ neurons (*w; Δhalo*). The antenna on the right contains $\Delta ab3A:Or7a$ neurons (*w; Δhalo; Or22a-GAL4/UAS-Or7a*).

(C) Odor response spectrum of control *ab3A* (first panel, *w*), $\Delta ab3A$ (second panel, *w; Δhalo*), $\Delta ab3A:Or7a$ (third panel, *w; Δhalo; Or22a-GAL4/UAS-Or7a*), and *ab4A* (fourth panel, *Canton-S*) neurons. For all graphs, *n* = 12.

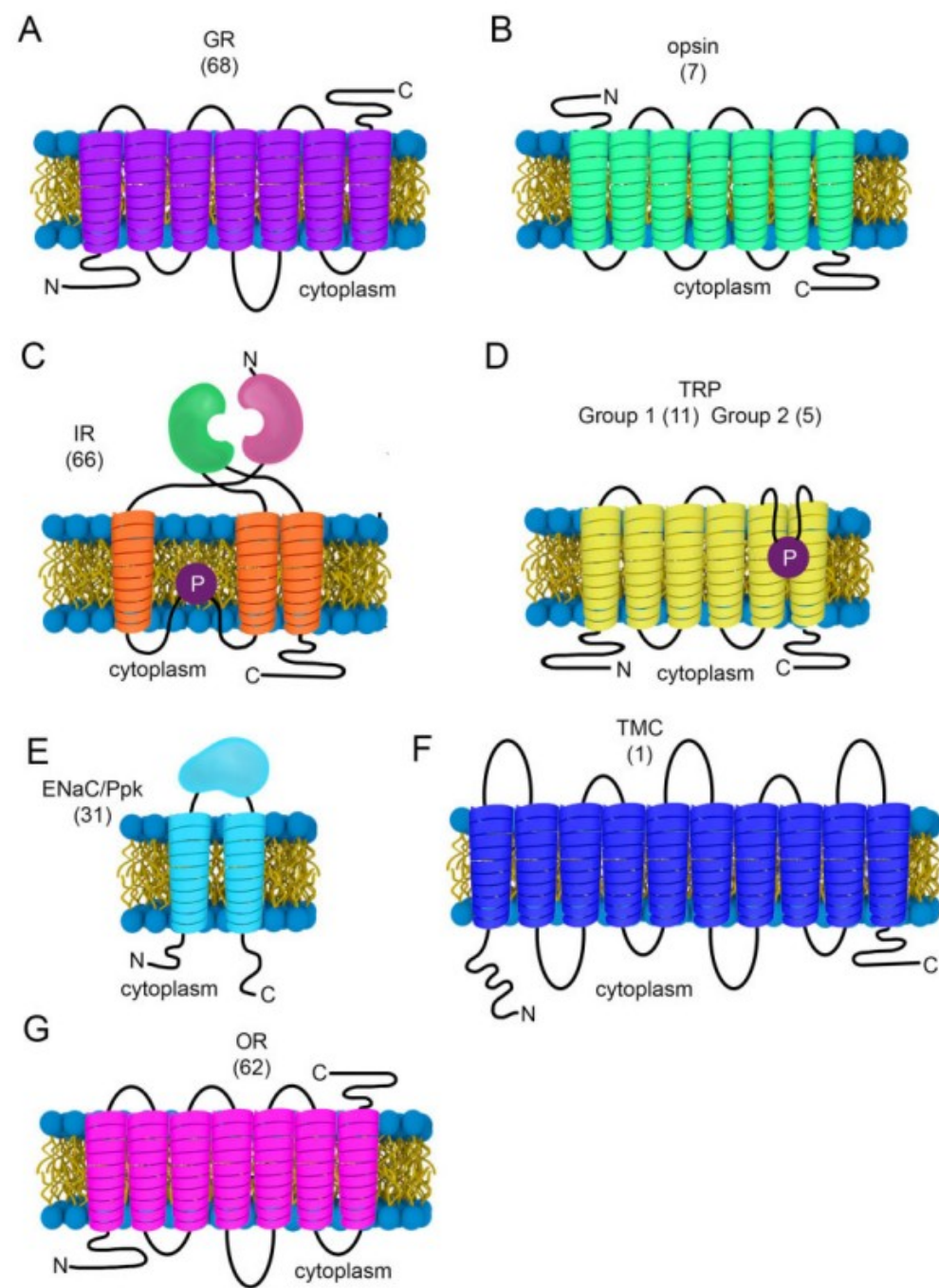


Figure 5. Transmembrane topologies of various sensory receptors and channels. The number of family members are indicated in brackets. (A) GR. (B) Opsin. (C) IR. (D) TRP. (E) ENaC/Ppk. (F) TMC. (G) OR. P, pore-loop.

1-octen-3-ol	•	•	+	•	++	++	•	—	++	+	•	+	—	•	•	•	+++	•	•	•	+++	•	—	+++
E2-hexenol	•	+++	++	—	+	+	•	•	++++	•	+	•	—	•	•	•	++	++	•	+	++++	+	•	++++
Z2-hexenol	•	+++	+	—	+	++	+	•	++++	+	+++	•	—	•	•	•	++	+	•	•	++	•	•	+
E3-hexenol	•	+++	+++	•	+	+	•	•	++++	•	+	•	—	•	•	•	+++	++	•	++	++++	+	—	++
Z3-hexenol	•	++	+++	•	+	•	•	•	++++	+	+	+	—	•	•	•	++	++	•	+	+++	+	—	++
glycerol	•	•	•	—	•	•	—	•	•	—	•	•	•	•	•	•	•	•	•	•	•	•	•	•
2,3-butanediol	•	—	++++	•	—	+	•	•	•	—	++	•	•	—	•	•	•	•	•	•	•	•	•	•
methyl acetate	•	•	•	•	•	+	•	•	•	—	•	•	•	—	++++	•	•	•	•	—	•	•	•	•
ethyl acetate	•	•	•	•	•	+	•	•	•	•	++	+	•	•	+++	•	•	•	•	+	•	•	•	•
propyl acetate	•	•	+++	+	•	+++	•	•	++	•	+++	++++	—	•	+	•	+	+	•	—	+++	•	•	+++
butyl acetate	+	—	+++	++	•	++++	•	•	+	•	++	++++	—	•	•	•	+++	•	•	—	++++	+	•	++++
pentyl acetate	•	•	+	•	++	+++	•	•	+++	•	+	++++	—	•	+	•	++++	•	•	•	+++	•	•	+++
hexyl acetate	•	—	•	—	+	+++	•	•	++++	•	•	++++	—	•	•	•	+	•	•	—	•	•	•	+
isobutyl acetate	•	•	+++	++++	•	++++	•	•	•	•	+++	+++	—	•	•	•	•	+	•	—	++	•	•	++++
isopentyl acetate	+	—	++	++++	+	++++	•	•	•	•	+	++	—	•	•	•	++	•	•	—	++++	•	•	++++
E2-hexenyl acetate	•	++++	•	•	•	+++	•	•	++++	—	•	+	—	•	•	•	+	•	•	•	•	•	•	++++
methyl butyrate	•	•	++	•	•	++++	•	•	++	•	+++	++	—	•	++	•	++	+	•	•	+	•	•	+
ethyl butyrate	•	•	++	•	+	+++	•	•	++	•	+++	+	•	•	•	+++	++	•	++	++	•	•	•	+
hexyl butyrate	•	•	•	•	•	•	•	•	++++	•	•	•	•	•	•	•	+	•	•	•	+	•	•	•
ethyl 3-hydroxybutyrate	+	—	++++	+	•	++	—	•	+	•	++	+	—	•	•	•	+	+	•	++++	++++	+	—	+++
ethyl propionate	•	+	+	•	•	+++	—	+	•	•	+++	+	•	—	+	•	•	•	•	•	+	•	•	•
ethyl methanoate	•	++	•	•	—	•	•	•	—	—	•	•	•	•	•	•	•	•	•	•	•	•	•	•
methyl hexanoate	•	•	+	•	•	++++	•	—	—	•	+	++++	—	•	•	•	+	•	•	—	++++	•	—	+++
ethyl hexanoate	•	—	•	—	•	++++	•	•	—	•	•	++	—	•	•	•	++	—	•	—	+	•	•	+
hexyl hexanoate	•	•	•	•	—	•	•	•	++	—	•	•	•	•	•	•	•	—	•	•	•	•	•	•
methyl octanoate	•	•	•	—	•	++++	•	•	•	—	•	+	—	•	•	•	—	•	•	—	+	•	•	•
ethyl octanoate	•	•	•	—	•	+	•	•	—	—	•	•	•	—	•	•	•	•	•	—	•	•	•	•
ethyl decanoate	•	—	•	•	—	•	•	•	—	•	•	•	•	•	•	•	—	—	•	—	•	•	•	•
ethyl trans-2-butenoate	•	•	++	++	•	++++	•	•	•	—	+++	•	—	•	•	•	++	•	•	+	+	•	•	++++
ethyl lactate	•	•	+	•	•	+	•	•	•	•	+	•	—	•	++	•	•	++++	•	•	+	+	•	+
diethyl succinate	•	—	•	—	•	++++	•	•	—	•	•	•	•	•	•	•	+++	•	•	—	•	•	•	•

Figure 1. Odor Responses

“•,” $n < 50$ spikes/s; “+,” $50 \leq n < 100$ spikes/s; “++,” $100 \leq n < 150$ spikes/s; “+++,” $150 \leq n < 200$ spikes/s; “++++,” $n \geq 200$ spikes/s; “—” indicates inhibition to a level $\leq 50\%$ of the spontaneous firing rate (Yao et al., 2005). Odorants are color coded by functional group (gold = amines, dark blue = lactones, pink = acids, black = sulfur compounds, light green = terpenes, gray = aldehydes, yellow = ketones, light blue = aromatics, red = alcohols, dark green = esters). In the case of odorants containing multiple functional groups, all odorants containing a phenol ring, a sulfur

Coding of Odors by a Receptor Repertoire

Elissa A. Hallem¹ and John R. Carlson^{1,*}

¹Department of Molecular, Cellular, and Developmental Biology, Yale University, New Haven, CT 06520, USA

*Contact: john.carlson@yale.edu

DOI 10.1016/j.cell.2006.01.050

SUMMARY


We provide a systematic analysis of how odor quality, quantity, and duration are encoded by the odorant receptor repertoire of the *Drosophila* antenna. We test the receptors with a panel of over 100 odors and find that strong responses are sparse, with response density dependent on chemical class. Individual receptors range along a continuum from narrowly tuned to broadly tuned. Broadly tuned receptors are most sensitive to structurally similar odorants. Strikingly, inhibitory responses are widespread among receptors. The temporal dynamics of the receptor repertoire provide a rich representation of odor quality, quantity, and duration. Receptors with similar odor sensitivity often map to widely dispersed glomeruli in the antennal lobe. We construct a multidimensional “odor space” based on the responses of each individual receptor and find that the positions of odors depend on their chemical class, concentration, and molecular complexity. The space provides a basis for predicting behavioral responses to odors.

sidered as a whole and analyzed with olfactory stimuli that vary widely in their features.

The fruit fly *Drosophila melanogaster* provides an excellent model system for the study of odor coding. Its olfactory system is similar in organization to that of other insects and vertebrates yet is small in size and easily amenable to molecular, genetic, and electrophysiological analysis (Hallem and Carlson, 2004). The *Drosophila* adult has two olfactory organs, the antenna and the maxillary palp, which contain only ~1200 and ~120 olfactory receptor neurons (ORNs), respectively (Shanbhag et al., 1999). The ORNs are found within sensory hairs called sensilla, of which there are three major morphological types: basiconic, coeloconic, and trichoid. Each sensillum contains the dendrites of up to four ORNs.

In both insects and mammals, activated ORNs produce sequences of action potentials that reflect the features of the odors that activate them (Bichao et al., 2003; de Bruyne et al., 1999, 2001; Duchamp-Viret et al., 1999; Heinbockel and Kaissling, 1996; Nikonov and Leal, 2002; Shields and Hildebrand, 2000; Stensmyr et al., 2003). The ORNs activate second-order neurons in the brain (Hildebrand and Shepherd, 1997). In *Drosophila*, extensive electrophysiological analysis of the antennal basiconic sensilla identified 18 functional classes of ORNs, which are found in stereotyped combinations within eight functional types of sensilla (de Bruyne et al., 2001; Elmore et al., 2003).

Drosophila sensory receptors—a set of molecular Swiss Army Knives

Craig Montell  *

Department of Molecular, Cellular, and Developmental Biology, The Neuroscience Research Institute, University of California, Santa Barbara, CA 93106, USA

*Address for correspondence: cmontell@ucsb.edu

Abstract

Genetic approaches in the fruit fly, *Drosophila melanogaster*, have led to a major triumph in the field of sensory biology—the discovery of multiple large families of sensory receptors and channels. Some of these families, such as transient receptor potential channels, are conserved from animals ranging from worms to humans, while others, such as “gustatory receptors,” “olfactory receptors,” and “ionotropic receptors,” are restricted to invertebrates. Prior to the identification of sensory receptors in flies, it was widely assumed that these proteins function in just one modality such as vision, smell, taste, hearing, and somatosensation, which includes thermosensation, light, and noxious mechanical touch. By employing a vast combination of genetic, behavioral, electrophysiological, and other approaches in flies, a major concept to emerge is that many sensory receptors are multitaskers. The earliest example of this idea was the discovery that individual transient receptor potential channels function in multiple senses. It is now clear that multitasking is exhibited by other large receptor families including gustatory receptors, ionotropic receptors, epithelial Na⁺ channels (also referred to as Pickpockets), and even opsins, which were formerly thought to function exclusively as light sensors. Genetic characterizations of these *Drosophila* receptors and the neurons that express them also reveal the mechanisms through which flies can accurately differentiate between different stimuli even when they activate the same receptor, as well as mechanisms of adaptation, amplification, and sensory integration. The insights gleaned from studies in flies have been highly influential in directing investigations in many other animal models.

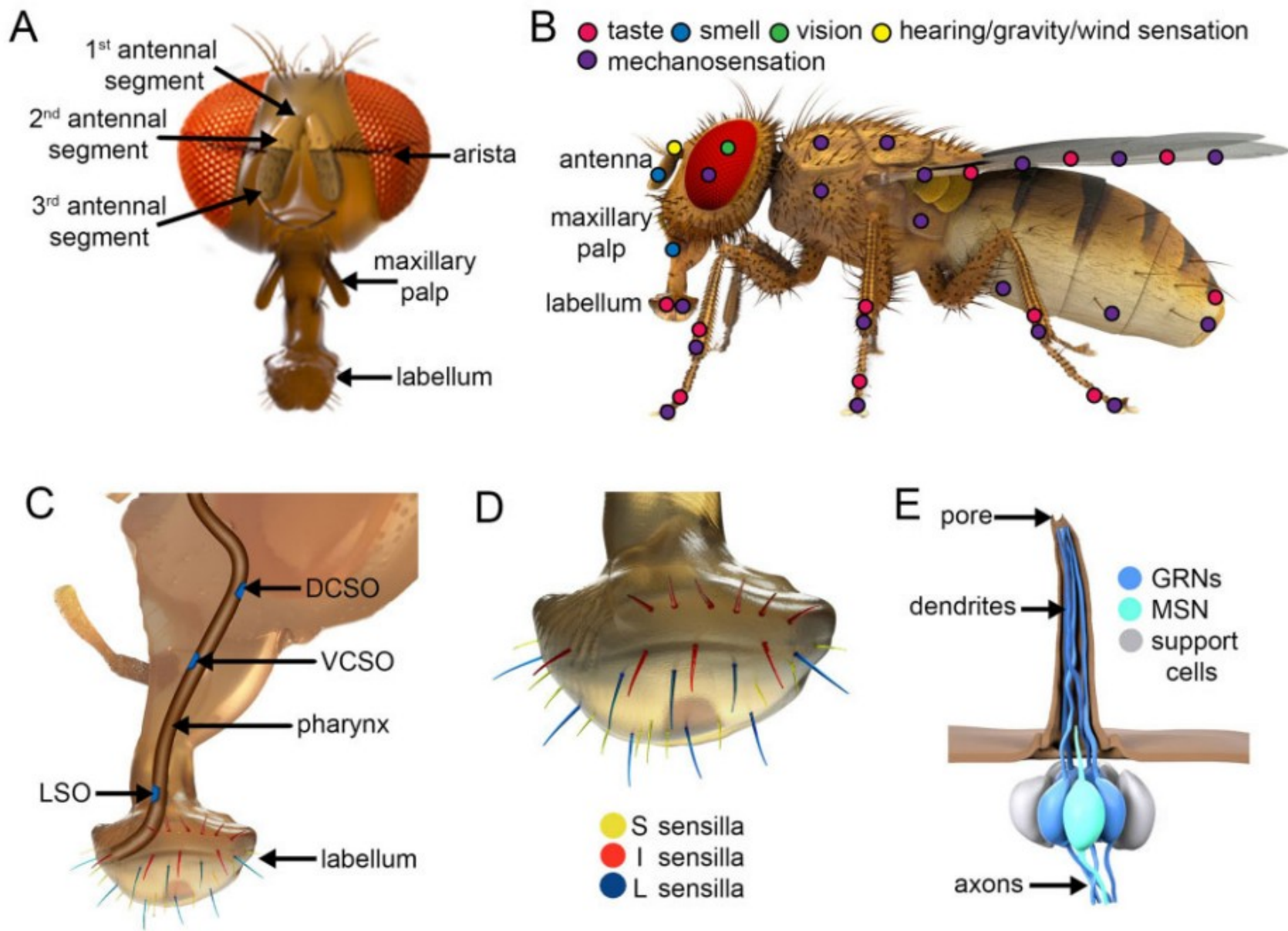


Figure 4. Sensory organs in adults. (A) Front view of a head. (B) Distribution of body parts that function in different senses. (C) Cutout from the side view of head showing the pharynx. Internal taste organs are indicated in blue: labral sense organs (LSOs), the dorsal cibarial sense organ (DCSO), and the ventral cibarial sense organ (VCISO). (D) S-, I- and L-type sensilla decorate the labellum. (E) An I-type taste sensillum showing two GRNs, the MSN, and support cells. The hair has a single pore at the distal end.

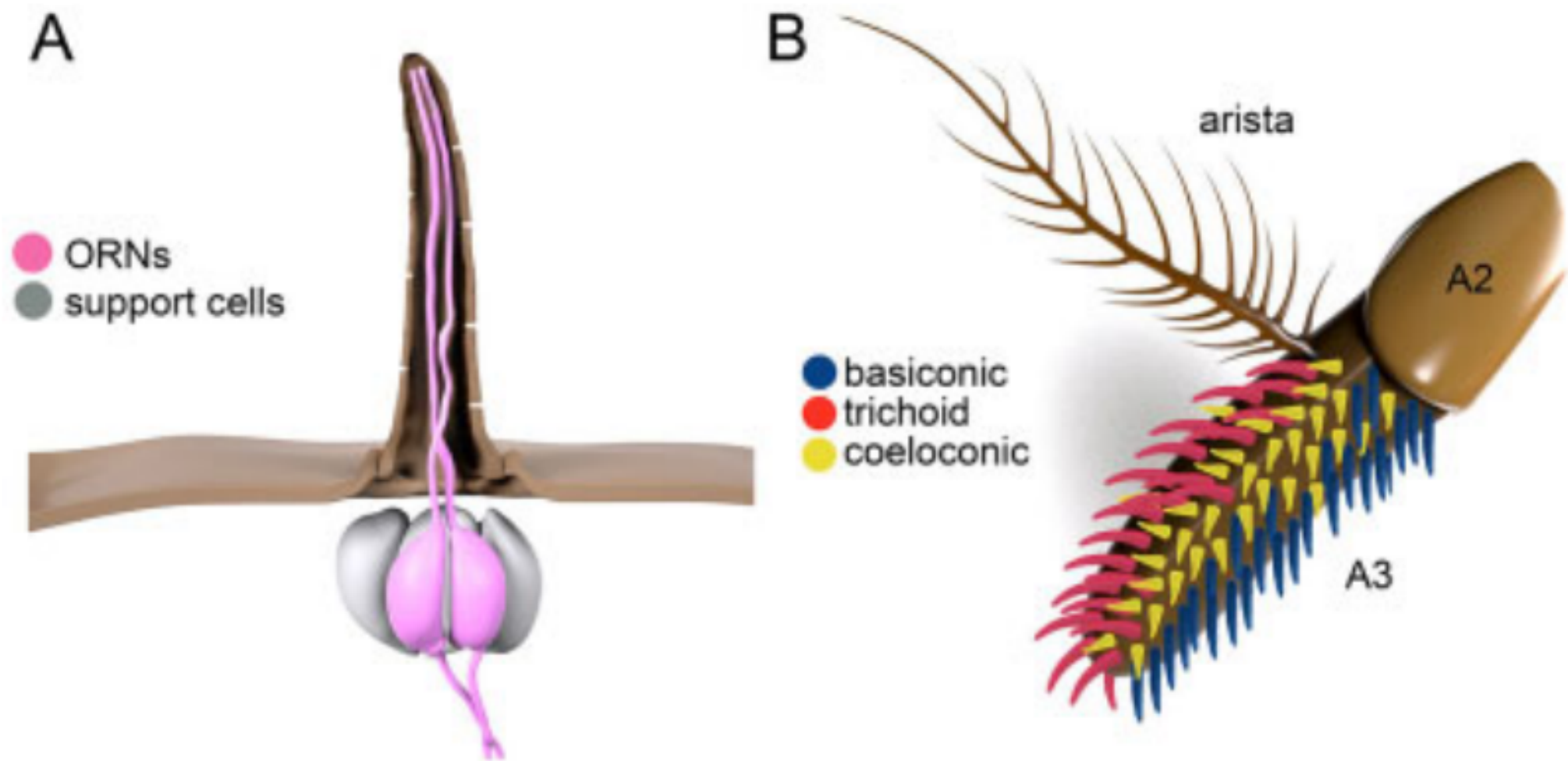


Figure 6. Olfactory sensilla. (A) Olfactory sensilla housing two neurons. The support cells and the distribution of pores are also indicated. (B) Antenna. The distributions of three types of olfactory sensilla are indicated. A2, second antennal segment; A3, third antennal segment.

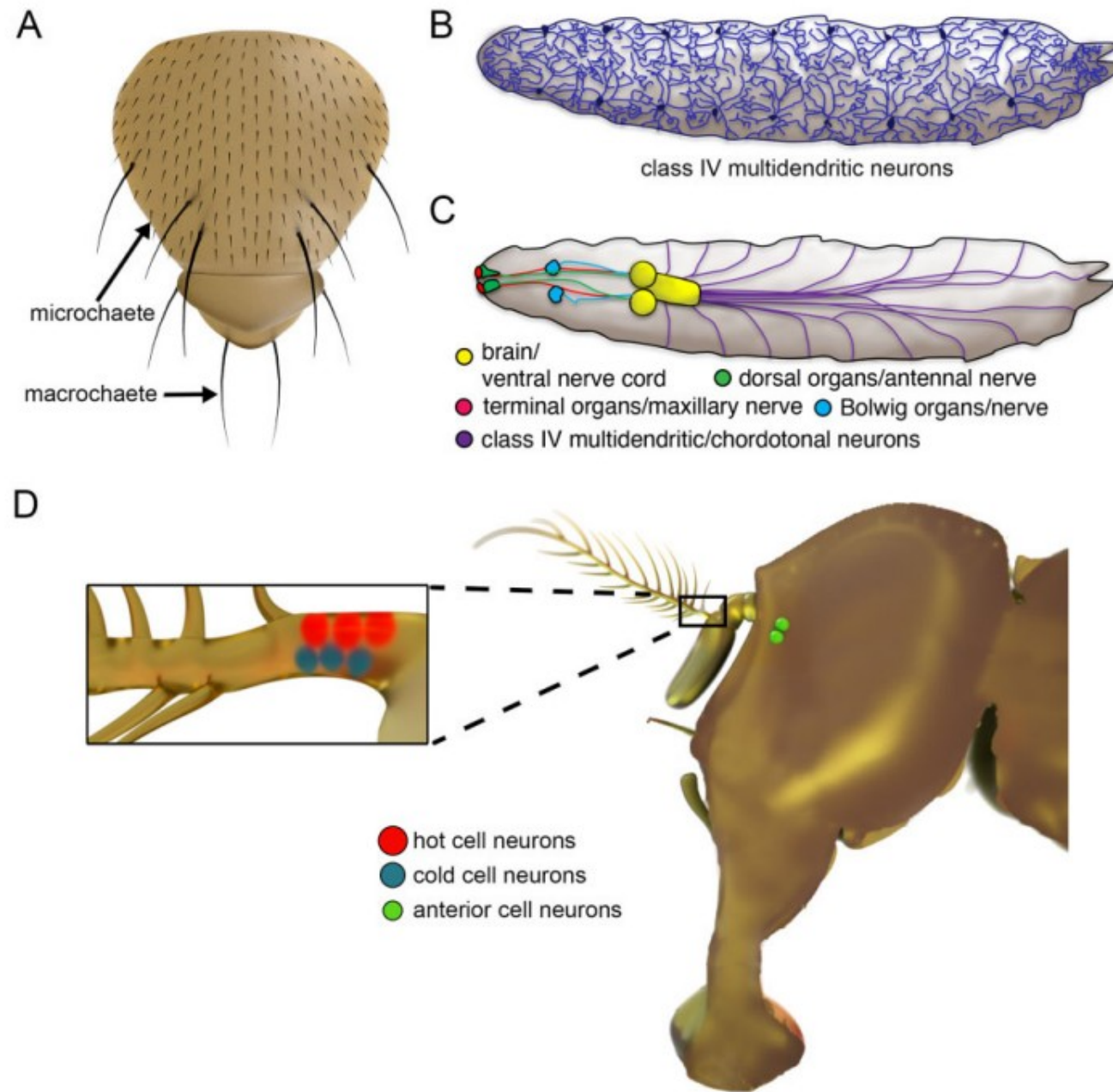


Figure 7. Mechanosensory sensilla on an adult thorax, thermosensory neurons in the arista, and sensory organs and neurons in larvae. (A) Distribution of microchaetae and macrochaetae on the adult thorax. (B) Arborization of class IV multidendritic neurons, which tile the body wall. (C) Sensory organs in larvae. (D) Side view of a head showing the positions of the anterior cell neurons in the brain (green) as well as the hot cell neurons (red cells) and cold cell neurons (blue) in the arista, a portion of which is magnified to the left.

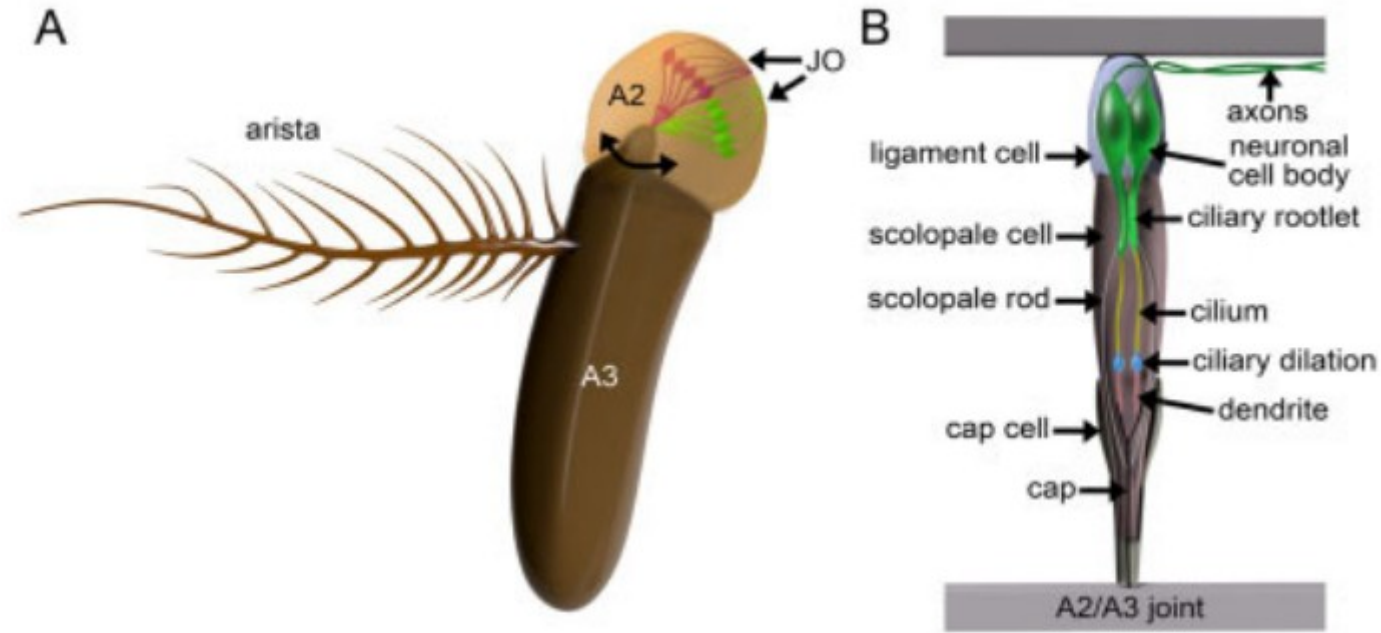


Figure 8. Auditory organ. (A) Antenna showing location of Johnston's organ (JO) in the 2nd antennal segment (A2). The arista and 3rd antennal segment are indicated. Shown are chordotonal neurons in the JO that function in detecting sound (purple) and wind/gravity (green). (B) A single scolopidium, which is the repeat unit in chordotonal organs such as the Johnston's organ. Each scolopidium in the JO is comprised of multiple cells including two neurons, a ligament cell, a scolopale cell, and a cap cell. The various parts of the neuron are indicated to the right.

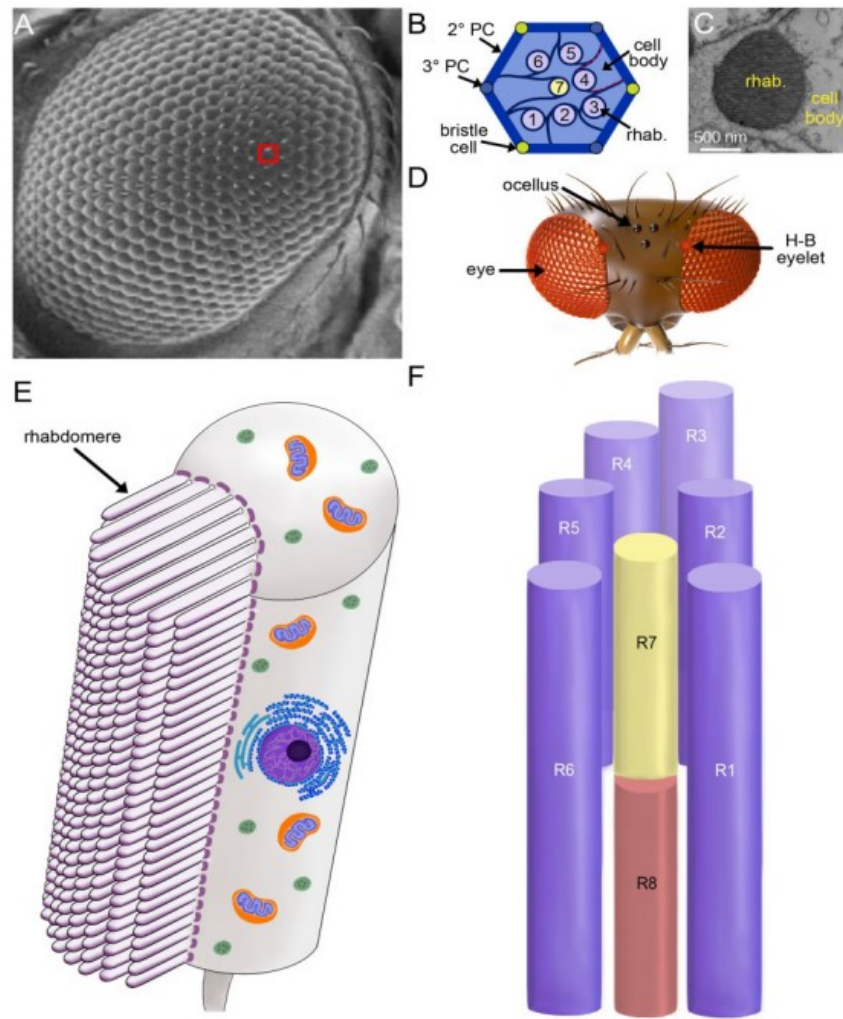


Figure 2. Light-sensitive organs and photoreceptor cells. (A) Scanning electron micrograph of an adult compound eye. The red square outlines one of the ~800 ommatidia. (B) Cartoon of a cross-sectional view through the distal region of an ommatidium. Shown are seven photoreceptor cells including the six outer photoreceptor cells, R1–6 (1–6), and the R7 photoreceptor (7). The circles represent the rhabdomeres. The red dashes outline the cell body of one photoreceptor cell (R4). 2° PC, secondary pigment cell; 3° PC, tertiary pigment cell; rhab., rhabdomere. (C) Transmission electron micrograph of a photoreceptor cell. (D) Cartoon of a top view of the head showing light-sensing organs. H-B, Hofbauer–Buchner. (E) Longitudinal representation of a single photoreceptor cell. The microvilli comprising the rhabdomere are indicated. Shown are far fewer microvilli than the 30,000–50,000 that normally comprise a rhabdomere. (F) Longitudinal view of the 8 rhabdomeres in a single ommatidium. The R1–6 cells extend the full depth of the retinal while the R7 and R8 cells occupy the distal and proximal regions of each ommatidium, respectively.

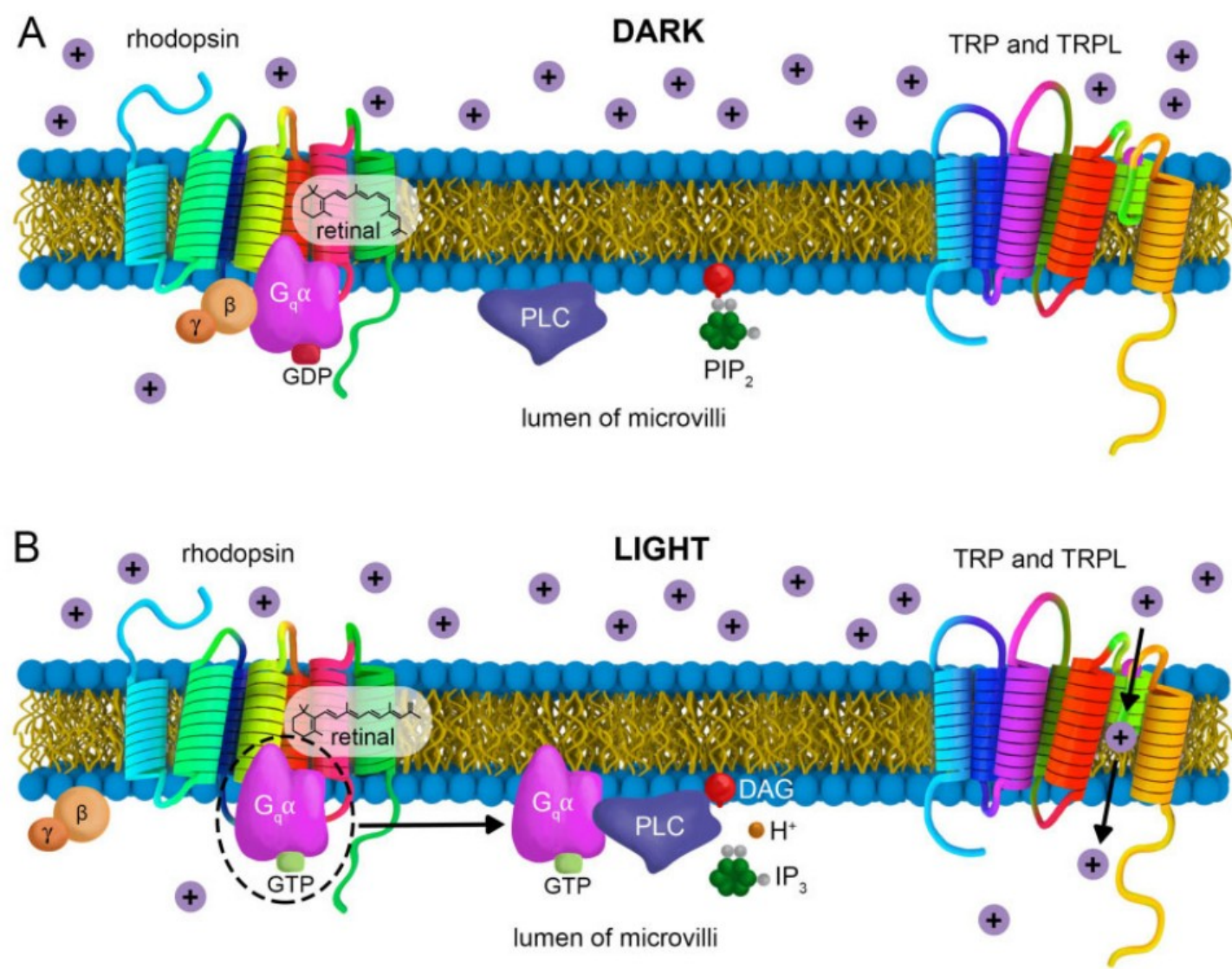


Figure 3. Phototransduction cascade. (A) Inactive (dark) state of the phototransduction cascade. Rhodopsin associates with 3-hydroxy 11-cis-retinal. The $G_q\alpha$ is bound to GDP and associates with $G\beta\gamma$. The TRP and TRPL channels are in the closed state. (B) Light-activated phototransduction cascade. Light induces the isomerization of 3-hydroxy 11-cis-retinal to 3-hydroxy all *trans*-retinal. This activates rhodopsin, causing an exchange of GTP for the GDP that was bound to the $G_q\alpha$, and dissociation of the $G\beta\gamma$. The $G_q\alpha$ -GTP is then released from rhodopsin, PLC is then activated, leading to hydrolysis of PIP_2 to create DAG, IP_3 , and H^+ . The cascade culminates with activation of TRP and TRPL and cation influx. The purple circles with a "+" represent cations (Na^+ or Ca^{2+}).

Table 1 Two groups and seven subfamilies of TRP channels

Group	Subfamily	Protein
1	TRPC	TRP TRPL TRP γ
1	TRPV	Nan Iav
1	TRPA	TRPA1 Pain Pyx WTRW
1	TRPM	TRPM
1	TRPN	NOMPC
2	TRPML	TRPML
2	TRPP	AMO (PKD2) Brv1 Brv2 Brv3

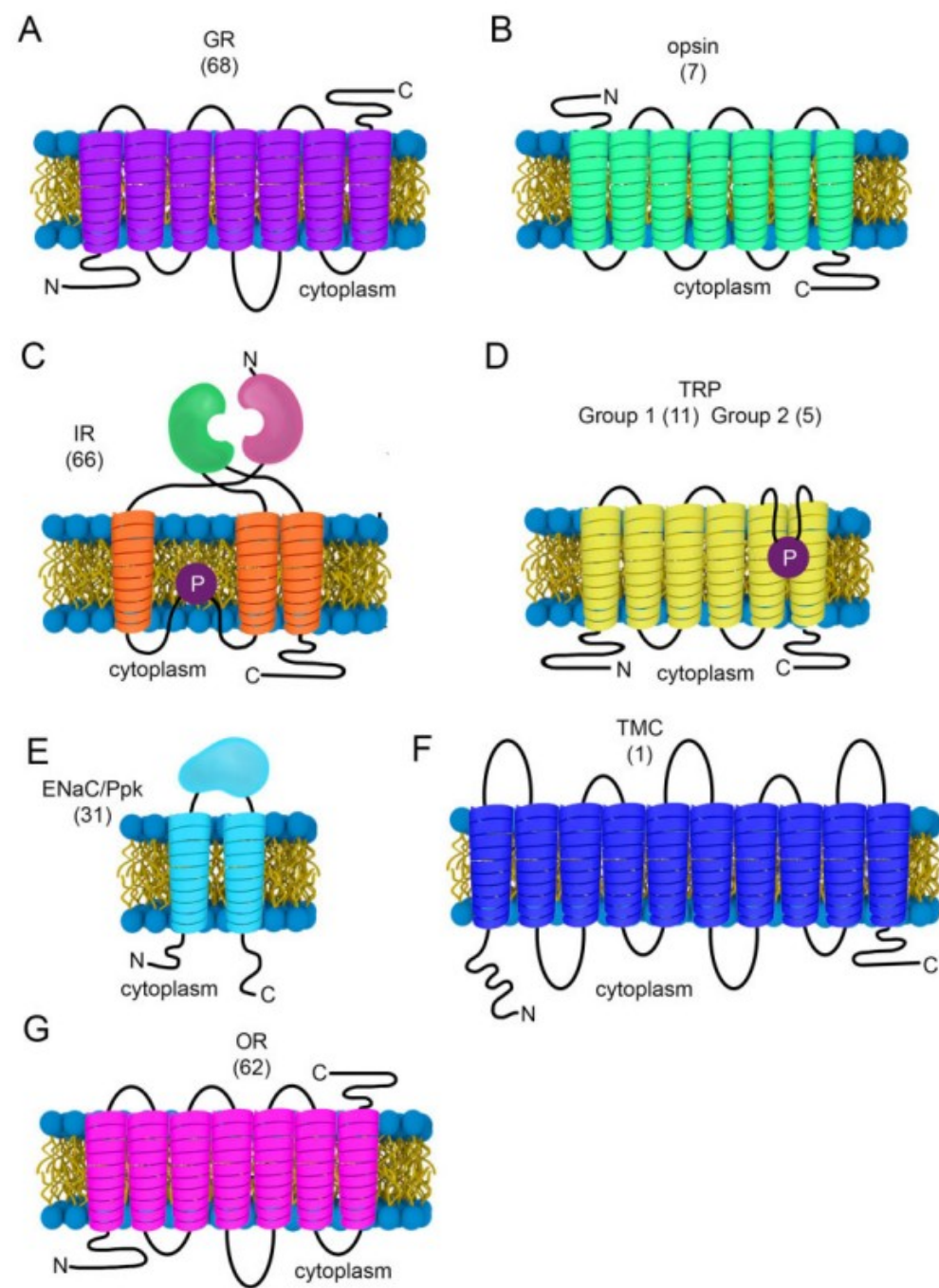


Figure 5. Transmembrane topologies of various sensory receptors and channels. The number of family members are indicated in brackets. (A) GR. (B) Opsin. (C) IR. (D) TRP. (E) ENaC/Ppk. (F) TMC. (G) OR. P, pore-loop.

Table 2 Types of GRNs in taste hairs

Sensilla	# GRNs	GRN	Markers	Former GRN names	Activators	Suppressors
S-type	4	A	Gr64f	“Sweet”	Sugars, low Na ⁺ , glycerol, fatty acids, acetic acid ^a	Bitter, Ca ²⁺ , acids
		B ^b	Gr66a	“Bitter”	Bitter, high Na ⁺ , acids, polyamines, tryptophan, L-canavanine, cool temperatures	
		C	Ppk28	“Water”	H ₂ O (hypo-osmolarity)	Osmolytes, salts (<i>e.g.</i> Na ⁺)
		D _s ^c	Ppk23, VGlut	“Cation”	High cations (<i>e.g.</i> Ca ²⁺ , Na ⁺ , K ⁺)	
I-type	2	A	Gr64f	“Sweet”	Sugars, low Na ⁺ , glycerol, fatty acids, acetic acid ^a	Bitter, Ca ²⁺ , acids
		B	Gr66a	“Bitter”	Bitter, acids, cool temperatures	
L-type	4	A	Gr64f	“Sweet”	Sugars, low Na ⁺ , glycerol, acetic acid ^a	Bitter, Ca ²⁺ , acids
		C	Ppk28	“Water”	H ₂ O (hypo-osmolarity)	
		D _L	Ppk23, VGlut	“Cation”	High cations (<i>e.g.</i> Na ⁺ , K ⁺)	Osmolytes, salts (<i>e.g.</i> Na ⁺)
		E	Ir94e	“Low salt”	Low Na ⁺	

^a A GRNs are more responsive to acetic acid in starved flies.

^b A subset of these B neurons are also positive for Ppk23 and ChAT.

^c These GRNs respond non-selectively to cations with particularly strong responses to Ca²⁺.

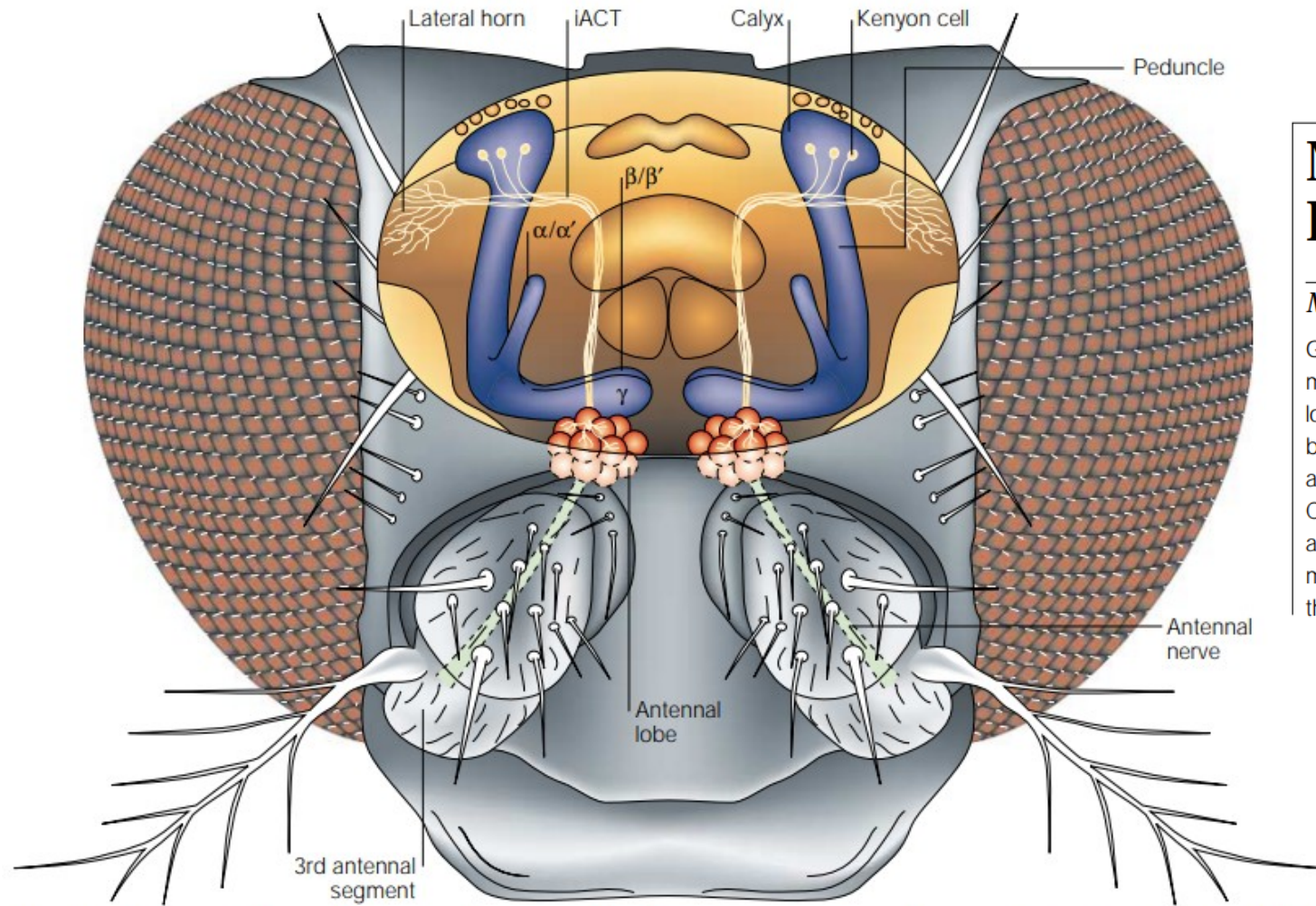


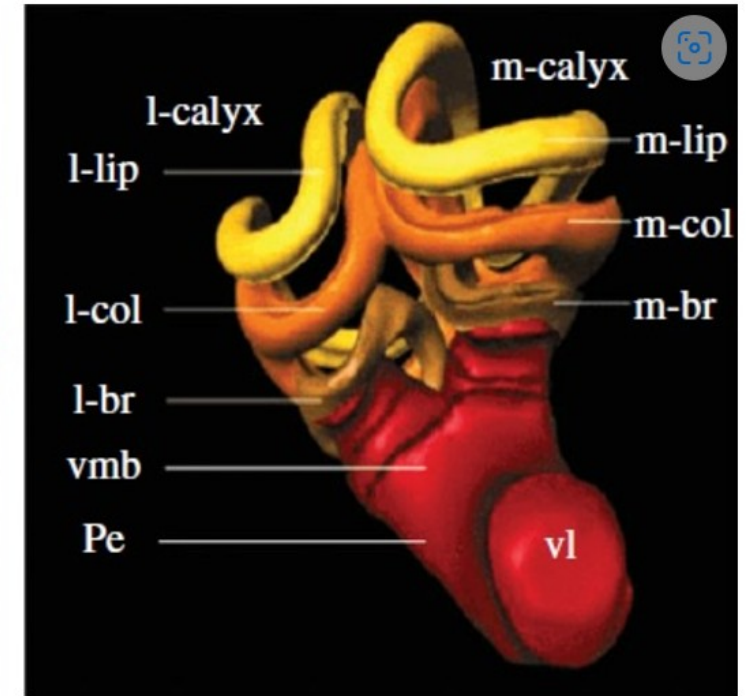
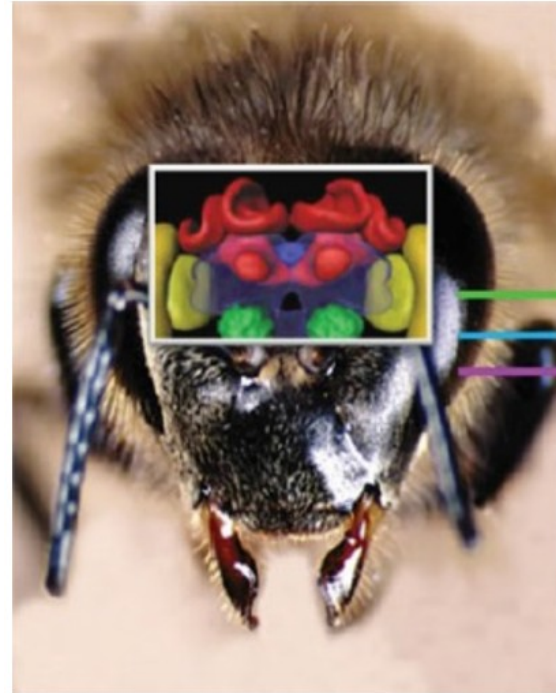
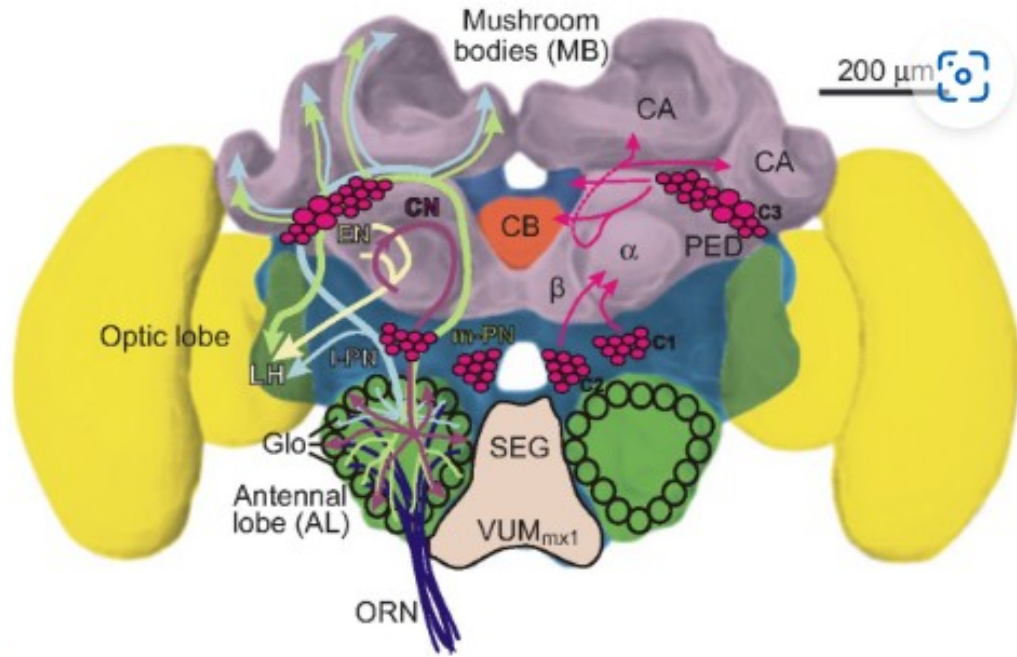
Figure 2 | **Olfactory pathway.** Odour information is carried from the third antennal segments and maxillary palps (not shown) to the antennal lobe, where receptor fibres are sorted according to their chemospecificities in about 40 glomeruli. These represent the primary odour qualities, which are reported to two major target areas in the brain, the dorsolateral protocerebrum (lateral horn) and the calyx of the mushroom body. The inner antennocerebral tract (iACT) connects individual glomeruli to both areas. α/α' , β/β' and γ mark the three mushroom body subsystems described by Crittenden *et al.* (REF. 64).

MUSHROOM BODY MEMOIR: FROM MAPS TO MODELS

Martin Heisenberg

Genetic intervention in the fly *Drosophila melanogaster* has provided strong evidence that the mushroom bodies of the insect brain act as the seat of a memory trace for odours. This localization gives the mushroom bodies a place in a network model of olfactory memory that is based on the functional anatomy of the olfactory system. In the model, complex odour mixtures are assumed to be represented by activated sets of intrinsic mushroom body neurons. Conditioning renders an extrinsic mushroom-body output neuron specifically responsive to such a set. Mushroom bodies have a second, less understood function in the organization of the motor output. The development of a circuit model that also addresses this function might allow the mushroom bodies to throw light on the basic operating principles of the brain.

Honeybee mushroom bodies, 200,000 Kenyon cells



Conditioned Behavior in *Drosophila melanogaster*

(learning/memory/odor discrimination/color vision)

WILLIAM G. QUINN, WILLIAM A. HARRIS, AND SEYMOUR BENZER

Division of Biology, California Institute of Technology, Pasadena, Calif. 91109

Contributed by Seymour Benzer, October 25, 1973

ABSTRACT Populations of *Drosophila* were trained by alternately exposing them to two odorants, one coupled with electric shock. On testing, the flies avoided the shock-associated odor. Pseudoconditioning, excitatory states, odor preference, sensitization, habituation, and subjective bias have been eliminated as explanations. The selective avoidance can be extinguished by retraining. All flies in the population have equal probability of expressing this behavior. Memory persists for 24 hr. Another paradigm has been developed in which flies learn to discriminate between light sources of different color.

larvae to oc interpreted shown to res

Nelson (1 conditioning testing indi we have sc *Drosophila* isolation, ir

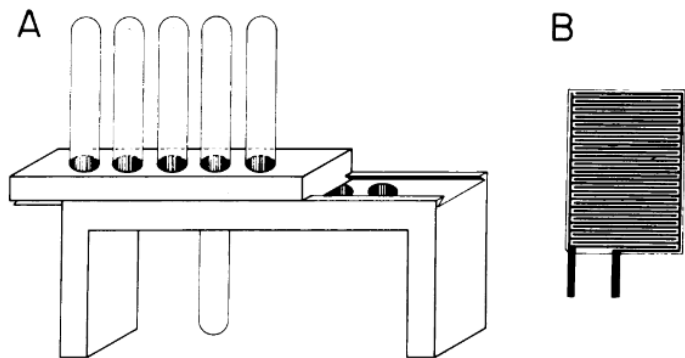


FIG. 1. (A) Apparatus used in the olfactory learning experiments. Two plastic blocks can be slid past each other on a dovetail joint. Holes running through each block are fitted with Teflon O-rings, to grip plastic tubes. (B) Printed circuit grid for shocking flies. The grid is rolled up and inserted into a plastic tube, which is plugged into the apparatus. Conductive tabs for applying voltage are bent around the tube rim to the outside.

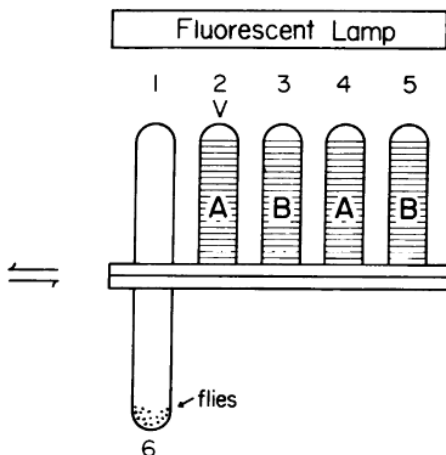


FIG. 2. Basic olfactory paradigm. Tube 1 is the rest tube, 2 and 3 are for training, 4 and 5 are for testing. Tube 6 is the start tube. Horizontal stripes in tubes indicate grids. A and B denote odorants 3-octanol and 4-methylcyclohexanol, respectively. V indicates voltage on the grid. See text for training and testing sequences.

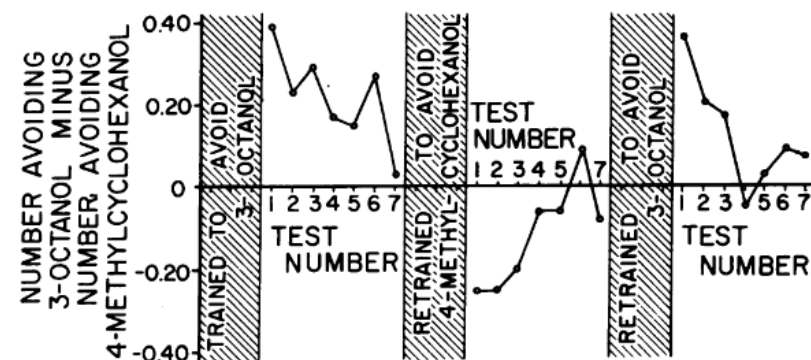


FIG. 3. Extinction and reversal of the learned response. A population of 36 flies was trained to avoid 3-octanol, then tested repeatedly without reinforcement. They were reverse-trained to avoid 4-methylcyclohexanol and retested, then reverse-trained and tested again.

In the basic paradigm (Fig. 2) tube 1 is a "rest" tube with holes at the end to allow odor to escape. Tubes 2-5 contain grids with odorants: tubes 2 and 4 each have 3-octanol on their grids; tubes 3 and 5 have 4-methylcyclohexanol. Tubes 2 and 3 are used for training, tubes 4 and 5 for testing. Voltage is applied to tube 2 only. The use of separate tubes for training and testing removes the flies from any odors they may have left on the grids during training, so that during testing the chemical odorants are the only possible cues for selective avoidance.

For training, the sequence of runs was: rest tube (60 sec), tube 2 (15 sec), rest tube (60 sec), tube 3 (15 sec). This cycle was repeated three times. (A tendency to avoid tube 2 was already evident by the second cycle.) The flies were then tested in the same sequence with tubes 4 and 5 instead of 2 and 3. The number of flies avoiding the grid on each run was counted visually. More flies avoided tube 4 than tube 5. Tube 4 contained 3-octanol, which had been presented simultaneously with shock during training.

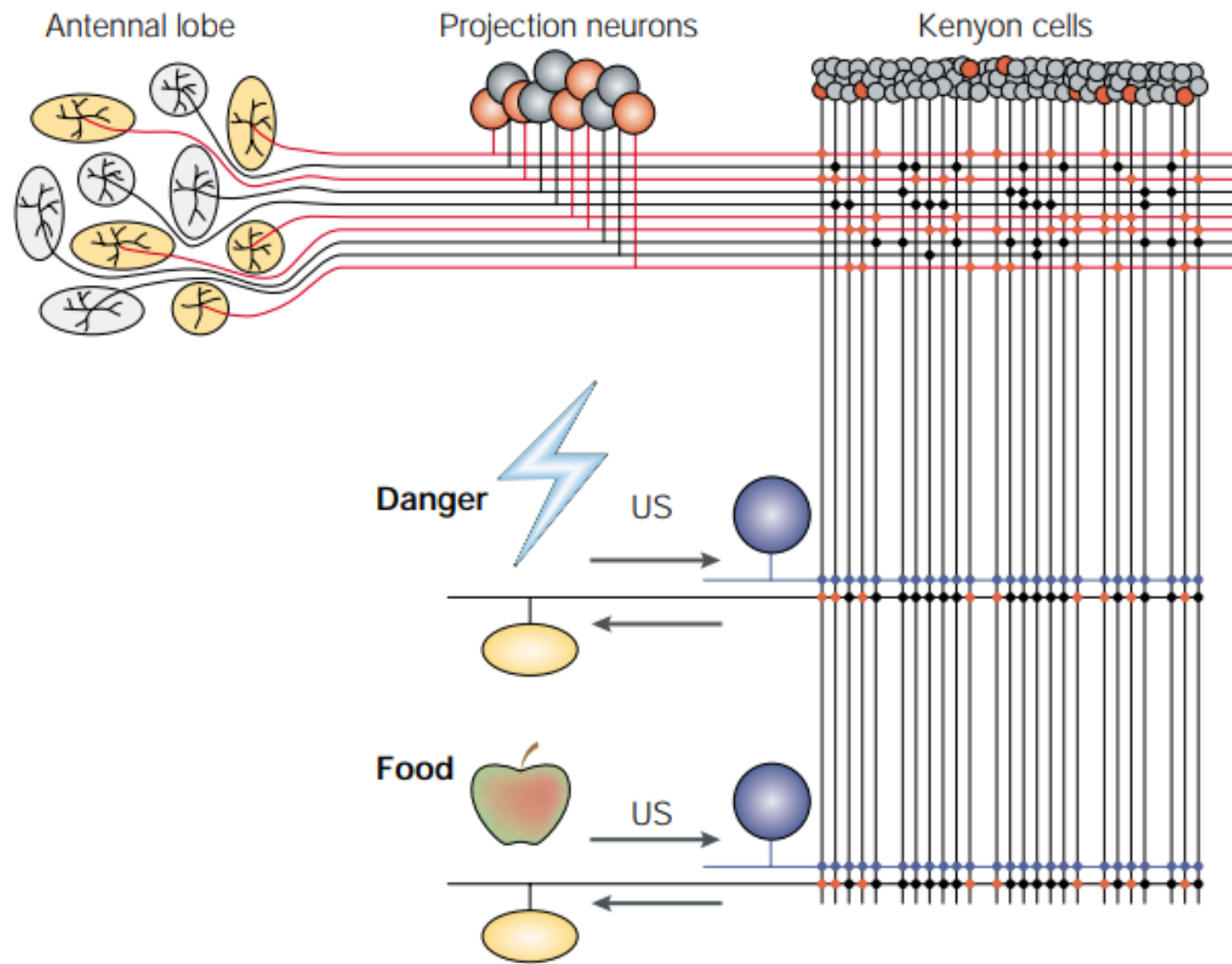
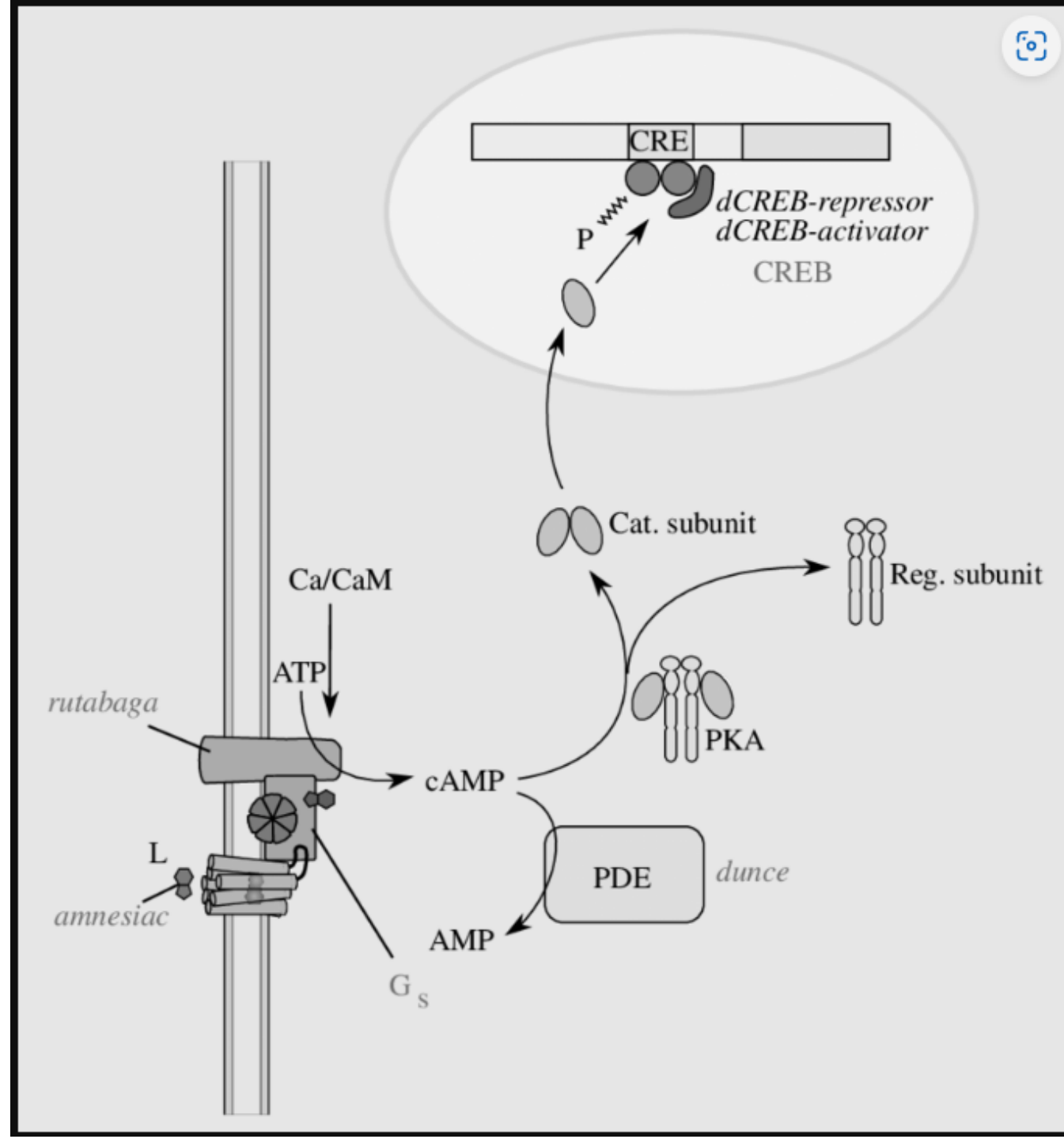


Figure 3 | **Circuit model of odour memory.** Odours are represented in the mushroom bodies by sets of Kenyon cells. Extrinsic mushroom-body output neurons are connected to the Kenyon cells by latent synapses. The output neurons are accompanied by modulatory input neurons presenting the unconditioned stimulus to the Kenyon cells. Simultaneous arrival of the conditioned (CS) and unconditioned stimulus (US) strengthens the synapses from Kenyon cells to output neurons (see also FIG. 4).

Box 2 | Number game

Let us assume that each Kenyon cell receives input from three primary odour qualities (POQs), each represented by a projection neuron. The Kenyon cell is activated only if all three input cells are active (coincidence detector). A hypothetical olfactory system with 40 POQs (only 10 are shown in FIG. 3) can form 9,216 triplets of POQs. (*Drosophila* has only 2,500 Kenyon cells, fewer than this scheme would require.) If an odour mixture A consists of 20 POQs, it will activate 1,035 Kenyon cells. If a second odour mixture B also has 20 POQs of which 10 are the same as in A, the two sets of Kenyon cells would overlap by only 11%. Two odours with 6 POQs each and 5 in common would each be represented by sets of 20 Kenyon cells, of which 10 would be activated by both odours. With a 50% overlap at the level of the POQs, the two sets of Kenyon cells would share only a single cell. The numbers show that because of the coincidence requirement, odour representations at the level of the mushroom body could be well separated.

Stupid fly mutants named after vegetables



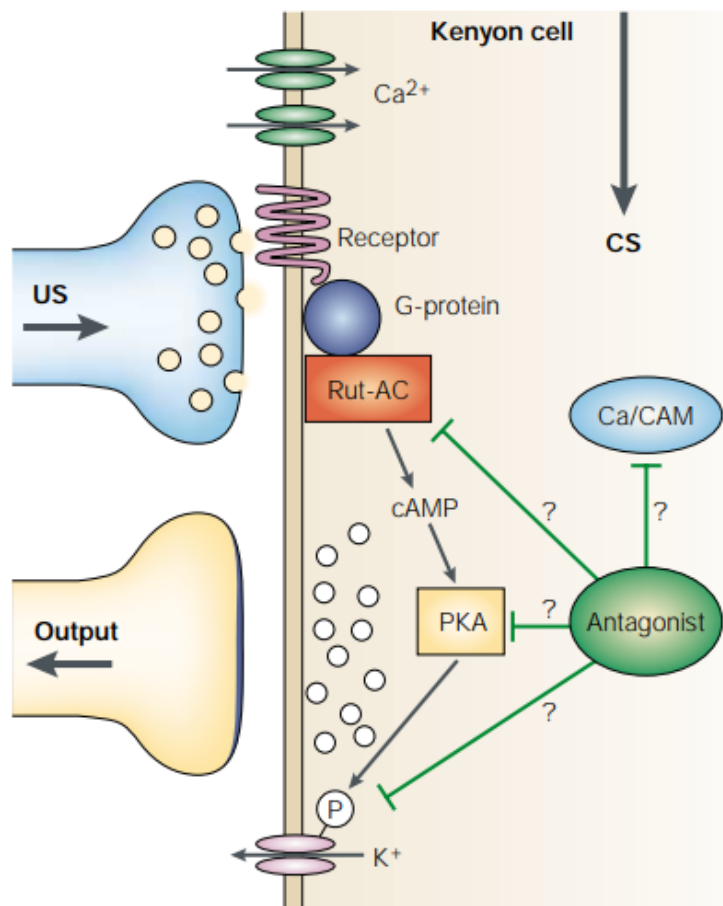


Figure 4 | **Presynaptic modulation of transmission at Kenyon cell-to-output neuron synapses is thought to underlie short- and middle-term memory of odours in flies.** Simultaneous arrival of the conditioned stimulus (CS) and the unconditioned stimulus (US) in the Kenyon cells activates adenylyl cyclase, which in turn increases cyclic AMP synthesis. Elevated levels of cAMP activate protein kinase A (PKA), which might phosphorylate target proteins at the synapse. To explain extinction, an antagonist is postulated that could interfere with any of the steps in the cAMP signalling pathway. Local, independently modulated synaptic domains for different USs might reside in the same Kenyon cells. Ca/CAM, calcium/calmodulin; Rut-AC, Ca/CAM-dependent adenylyl cyclase. Adapted, with permission, from REF. 36 © (2002) Elsevier Science.

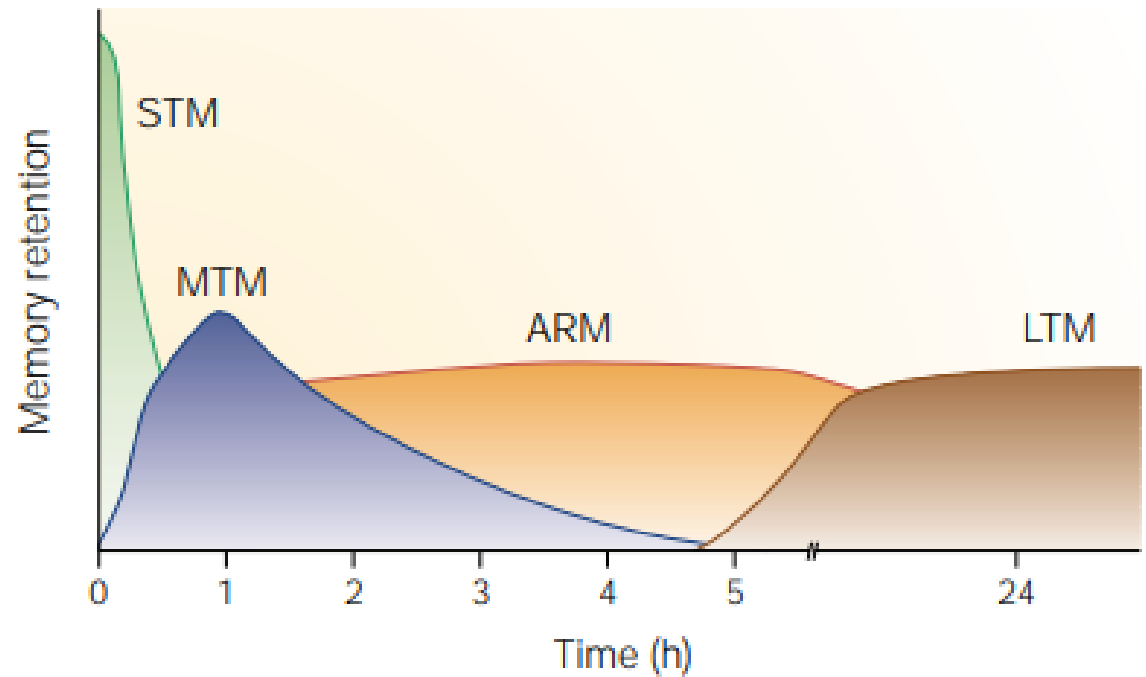


Figure 5 | **Memory phases after electric-shock conditioning.** Long-term memory (LTM) extends beyond two days and requires protein synthesis. Anaesthesia-resistant memory (ARM) is found together with LTM at 24h, does not require protein synthesis and cannot be erased by anaesthesia after memory consolidation. Middle-term memory (MTM), if it is a separate memory phase, can be observed in a mutant lacking ARM (*radish*) between one and three hours after training. Short-term memory (STM) remains in mutants lacking the *amnesiac* gene, which is required for MTM, ARM and LTM. Adapted, with permission, from REF. 65 © (1995) Elsevier Science.

Learning and memory using *Drosophila melanogaster*: a focus on advances made in the fifth decade of research

Ronald L. Davis*

Department of Neuroscience, Herbert Wertheim UF Scripps Institute for Biomedical Innovation & Technology, University of Florida, 130 Scripps Way, Jupiter, FL 33458, USA

*Corresponding author: Email: ronaldldavis@ufl.edu

Abstract

In the last decade, researchers using *Drosophila melanogaster* have made extraordinary progress in uncovering the mysteries underlying learning and memory. This progress has been propelled by the amazing toolkit available that affords combined behavioral, molecular, electrophysiological, and systems neuroscience approaches. The arduous reconstruction of electron microscopic images resulted in a first-generation connectome of the adult and larval brain, revealing complex structural interconnections between memory-related neurons. This serves as substrate for future investigations on these connections and for building complete circuits from sensory cue detection to changes in motor behavior. Mushroom body output neurons (MBO_n) were discovered, which individually forward information from discrete and non-overlapping compartments of the axons of mushroom body neurons (MB_n). These neurons mirror the previously discovered tiling of mushroom body axons by inputs from dopamine neurons and have led to a model that ascribes the valence of the learning event, either appetitive or aversive, to the activity of different populations of dopamine neurons and the balance of MBO_n activity in promoting avoidance or approach behavior. Studies of the calyx, which houses the MB_n dendrites, have revealed a beautiful microglomerular organization and structural changes of synapses that occur with long-term memory (LTM) formation. Larval learning has advanced, positioning it to possibly lead in producing new conceptual insights due to its markedly simpler structure over the adult brain. Advances were made in how cAMP response element-binding protein interacts with protein kinases and other transcription factors to promote the formation of LTM. New insights were made on Orb2, a prion-like protein that forms oligomers to enhance synaptic protein synthesis required for LTM formation. Finally, *Drosophila* research has pioneered our understanding of the mechanisms that mediate permanent and transient active forgetting, an important function of the brain along with acquisition, consolidation, and retrieval. This was catalyzed partly by the identification of memory suppressor genes—genes whose normal function is to limit memory formation.

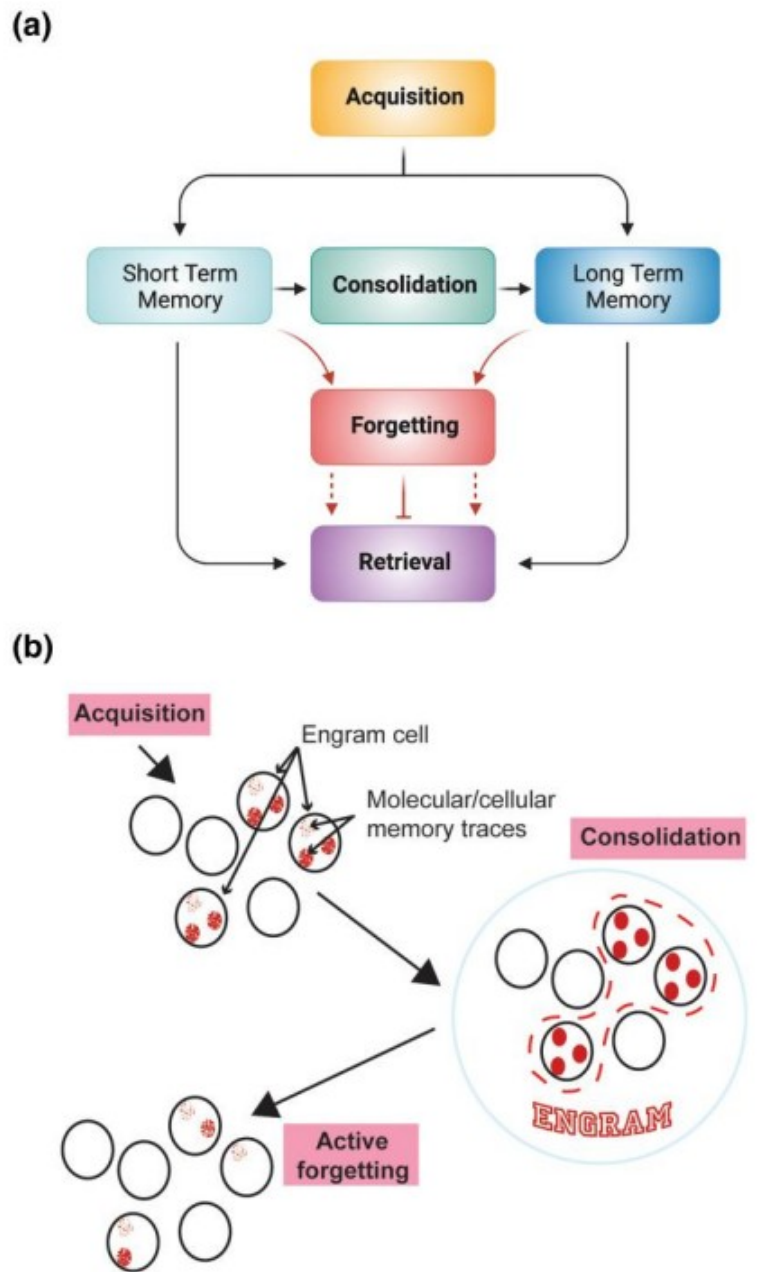


Fig. 1. a) The nervous system uses four operations for short- and long-term memory formation: acquisition, consolidation, forgetting, and retrieval. Acquisition is synonymous with “learning,” and represents the initial encoding of information. Consolidation refers to the processes

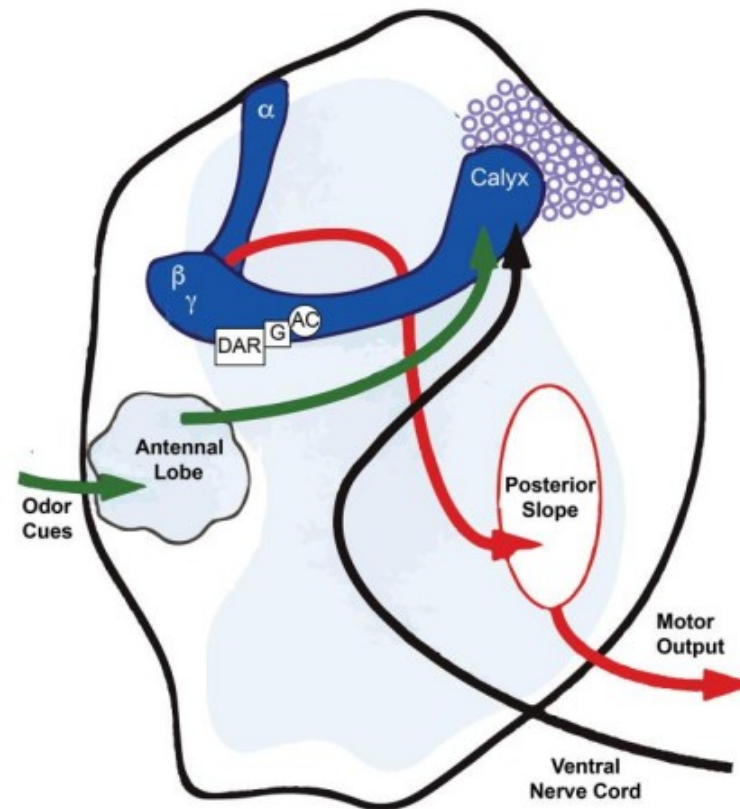


Fig. 2. Early model for olfactory learning envisioning odor cues being communicated to the MBn via the antennal lobe, and aversive shock information being communicated to the MBn via an ascending pathway from the ventral nerve cord. The MB includes the cell bodies (purple circles), the dendritic region (calyx), and the axons distributed into neuropil regions called lobes (α, β, γ lobes). The α -lobes project dorsally, and the β and γ lobes project medially. The *rutabaga*-encoded adenylyl cyclase and its associated G-protein (G) was envisioned to be coupled to a neuromodulatory receptor, probably dopamine (DAR), to help integrate the CS and US signals. This would lead to altered behavior in response to the CS from altered motor output instructions to the thoracic ganglia. Reproduced with permission from Davis 1993.

The identification and characterization of single gene mutations that impair learning and memory began shortly after behavioral assays were developed. Multiple ways were employed to create single gene mutants, including chemical mutagenesis, transposon mobilization, and enhancer detection (reviewed by Quinn and Greenspan 1984; Davis 1993; and Waddell and Quinn

(b)

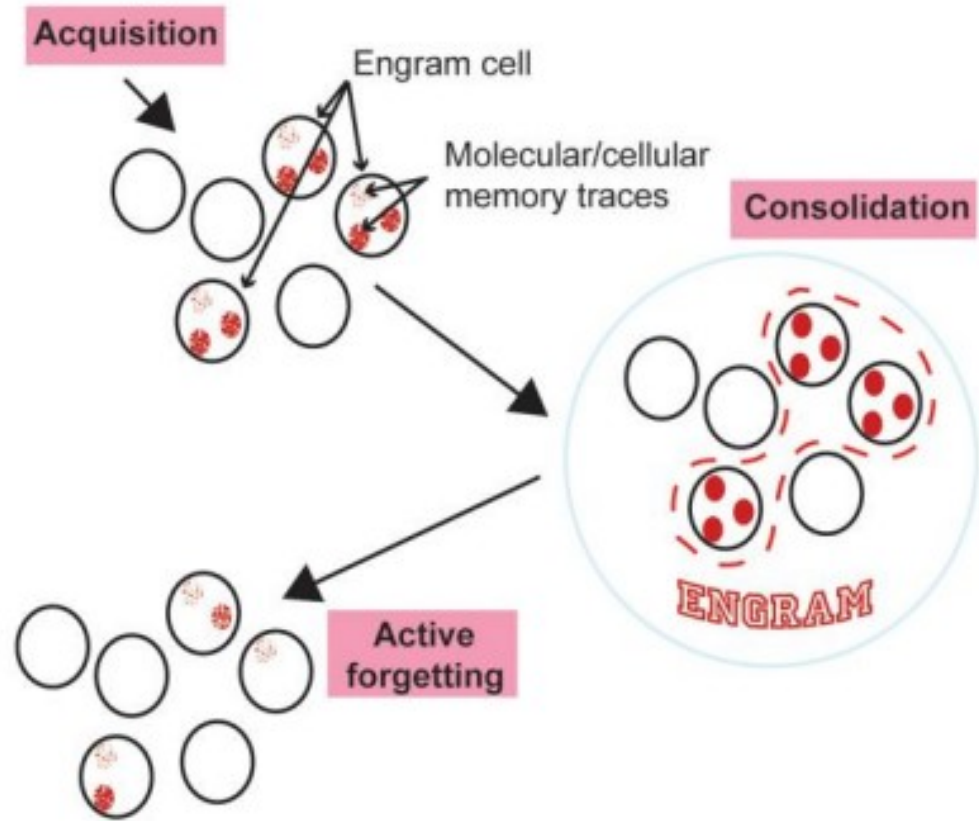
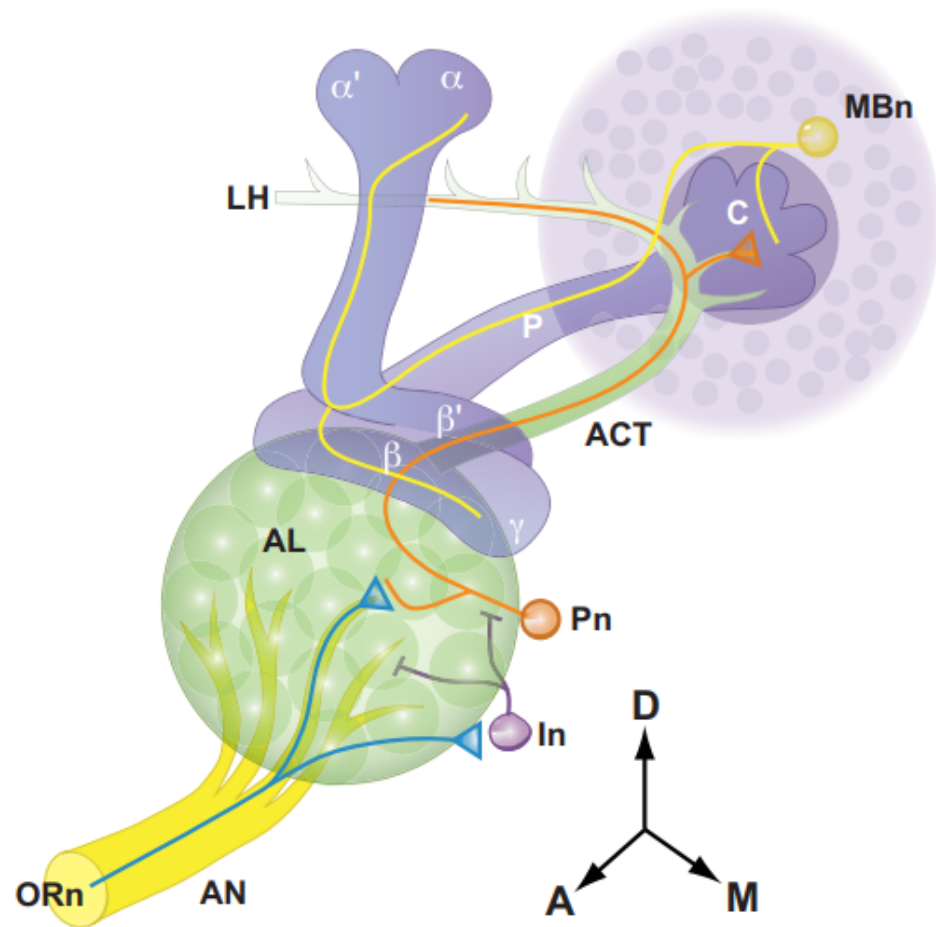


Fig. 1. a) The nervous system uses four operations for short- and long-term memory formation: acquisition, consolidation, forgetting, and retrieval. Acquisition is synonymous with “learning,” and represents the initial encoding of information. Consolidation refers to the processes involved in stabilizing memory over time. Forgetting involves mechanisms whereby memories can be erased or hidden from retrieval. Retrieval is simply the recollection, or recall, of existing memories. b) Cartoon illustrating the broad cellular and network events of memory formation. During acquisition, selected cells in the nervous system undergo molecular or biochemical changes that alter their physiological state. These selected cells are known as engram cells, and the molecular or biochemical changes within the engram cells are termed molecular or cellular memory traces. Consolidation mechanisms stabilize the cellular memory traces and the selected engram cells, together with their corresponding memory traces, represent the overall “engram” for a given memory. The activity of forgetting cells can erode the memory traces and cause memory failure. Modified with permission from [Noyes et al. 2021](#) and [Davis and Zhong 2017](#).

(a)



(b)

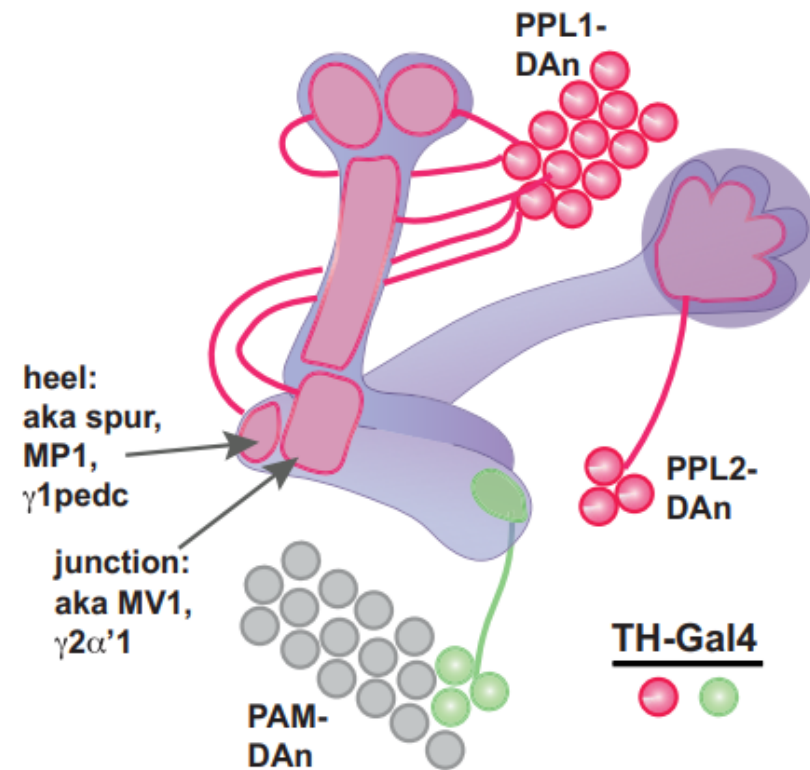


Fig. 3. a). Structure of the olfactory nervous system. Olfactory information is communicated to the MBn from the olfactory receptor neurons (ORN) on the antennae, to the projection neurons (Pn) in the antennal lobe (AL), whose axons comprise the antennal cerebral tract (ACT), to the dendrites of the MBn in the calyx (C). The ACT continues beyond the calyx to the lateral horn (LH). The AL also contains GABAergic interneurons (In) that help shape information processing. The MBn extend their primary axons through the peduncle (P) to the vertical and horizontal lobes. The α/β MBn send axon branches into both the vertical (α) and horizontal (β) lobes. This arrangement is mirrored by the α'/β' MBn (α' vertical and β' horizontal lobes). The axons of the γ MBn extend only into the horizontal γ lobe. Reproduced with permission from Davis 2011. b) Innervation pattern of the MB neuropil by DAN that are labeled by the TH-Gal4 driver. Three clusters of DAN—PPL1, PPL2, and PAM—send axon projections into the MB neuropil. The 12 PPL1-DAN innervate defined segments (compartments) of the vertical lobes, the junction area, and the heel. The junction and heel compartments have alternative names as indicated in the figure. PPL2-DAN innervate the calyx. Only a small number of PAM-DAN express the TH-Gal4 driver. Other PAM-DAN innervate compartments of the horizontal lobes. Modified with permission from Boto et al. 2019.

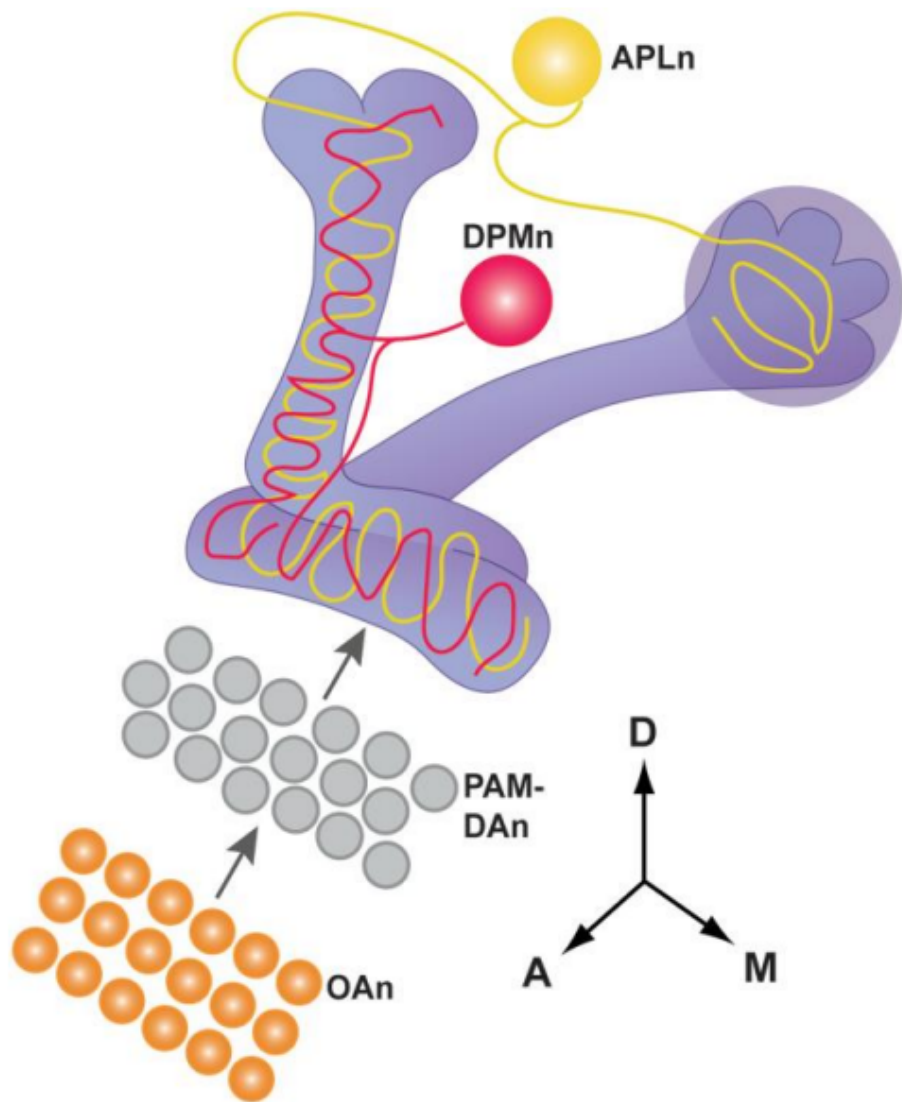


Fig. 5. Figure showing other classes of neurons in addition to the DAN (fig. 3b) that innervate the MB neuropil. There is a single DPMn per hemisphere that broadly innervates the vertical and horizontal lobes. The single APLn per hemisphere also broadly innervates the lobes and the calyx. The layering of PAM-DAN between OAn and the MB horizontal lobe is depicted. Modified with permission from [Güven-Ozkan and Davis \(2014\)](#).

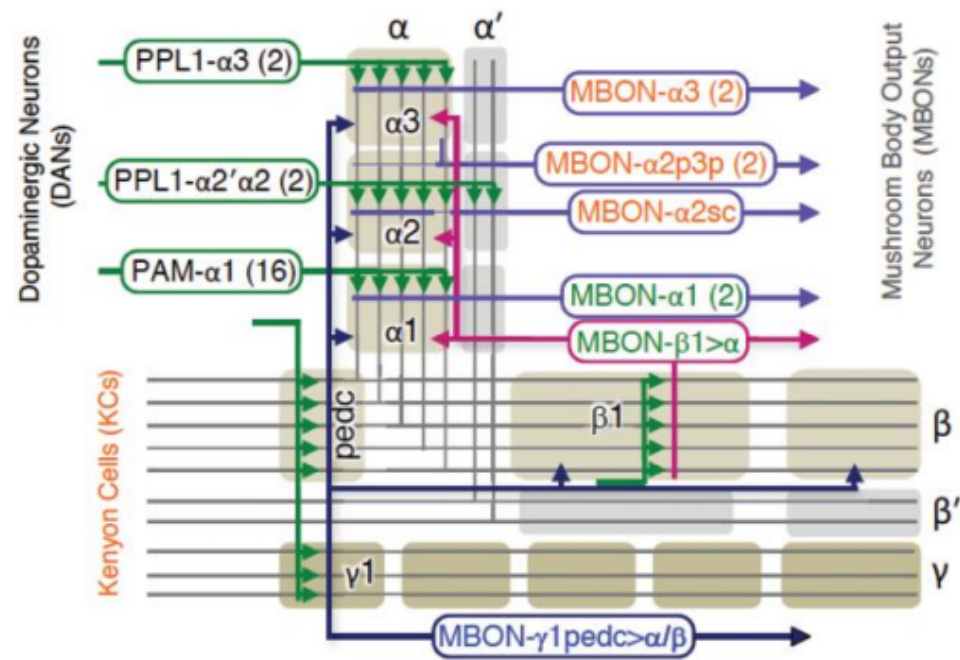
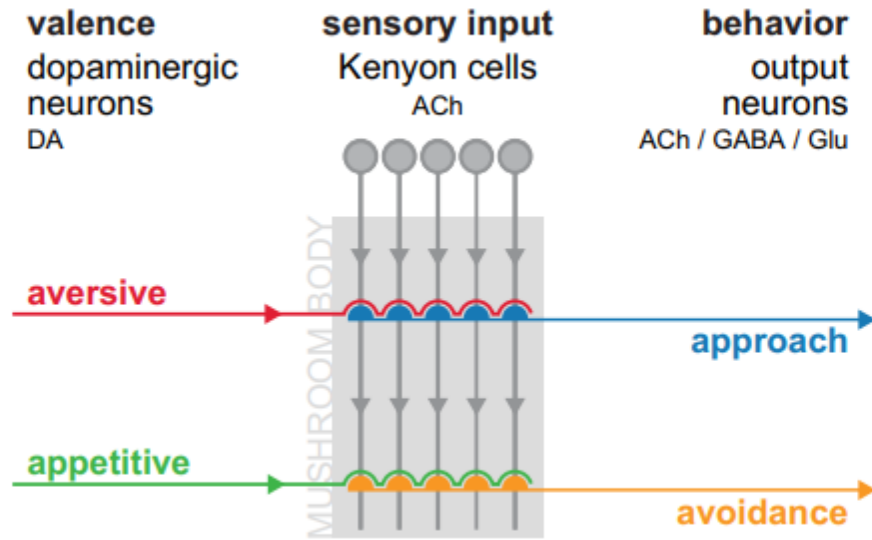


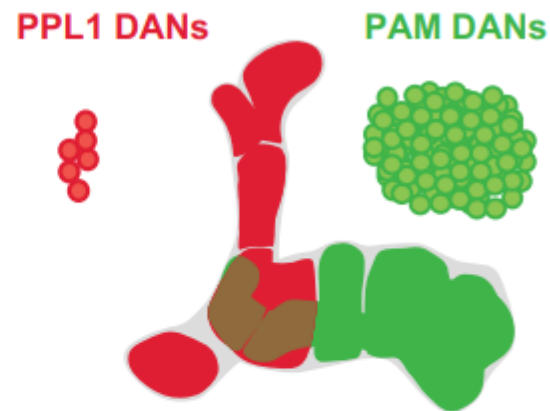
Fig. 6. Subway map showing the compartment organization of MBn axons, illustrating the 3 major classes of MBn (α/β , α'/β' and γ MBn), compartment (gray and tan shading) specific input from PPL1 and PAM clusters of DAN, and compartment specific output from MBON's. This figure focuses on the inputs and outputs from the vertical lobe compartments of α/β MBn, but a similar compartment and input (DAN) and output (MBON) arrangement exists for the horizontal lobes (see [Fig. 7b](#)). Reproduced with permission from [Takemura et al. 2017](#).

acquisition, providing serotonergic feedback to MBn to constrain the time window needed for CS/US associations to occur ([Zeng et al. 2023](#)). DAN exist in multiple clusters in the brain with two clusters, PPL1 and PAM, responsible for DA input onto the MBn axons in the vertical and horizontal lobes, respectively, as discussed above. The ~22 different types of DAN tile the MB axons into 15 compartments, with individual DAN innervating a single or some-

(a)



(b)



(c)

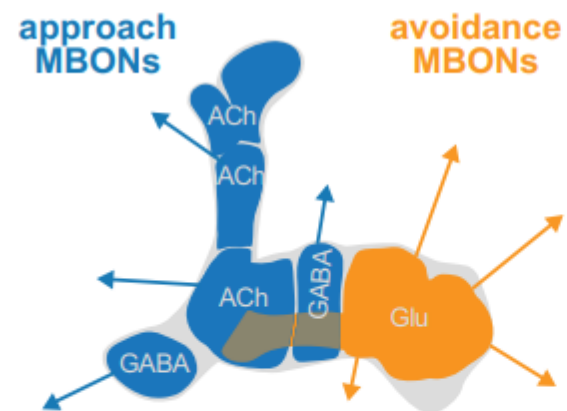


Fig. 7. a) DAN in the PPL1 cluster provide aversive information to the MBn axons in the vertical lobe compartments, while DAN in the PAM cluster provide primarily appetitive information to the horizontal lobe compartments. This valence is integrated with odor information carried by the MBn axons and conveyed to the MBO. Aversive signals decrease the activity of “approach” MBO, while appetitive signals decrease the activity of “avoidance” MBO. b) Color map showing the compartments innervated by PPL1- and PAM-DAN. c) Color map indicating the neurotransmitter phenotype of the compartment specific MBO. Reproduced with permission from [Cognigni et al., 2018](#).

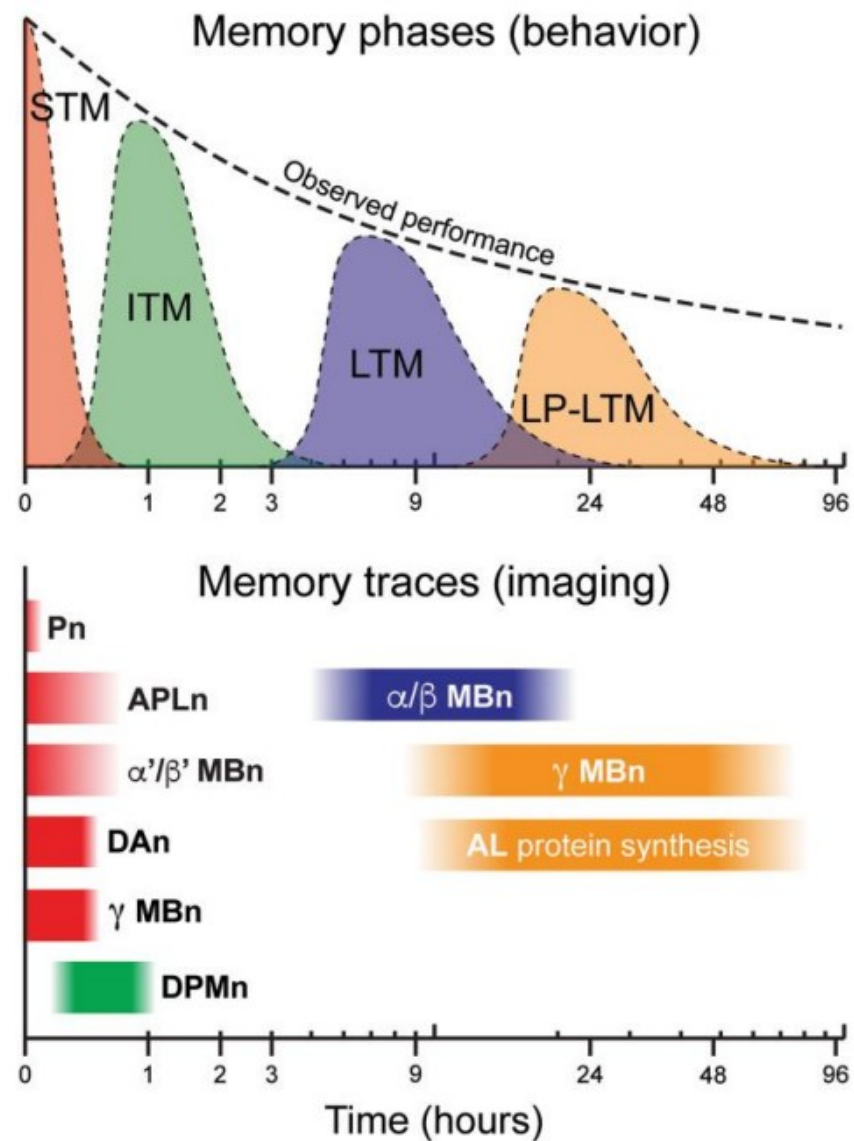


Fig. 8. Memory phases and cellular memory traces. Behavioral memory expression is the combination of separate memory phases: short-term memory (STM), intermediate-term memory (ITM), long-term memory (LTM), and late-phase long-term memory (LP-LTM). Cellular memory traces have been found in Pn, APLn, α'/β' MBn, DPMn, α/β MBn, γ MBn, DAn, and MBOn. Modified with permission from Tomchik and Davis 2013.

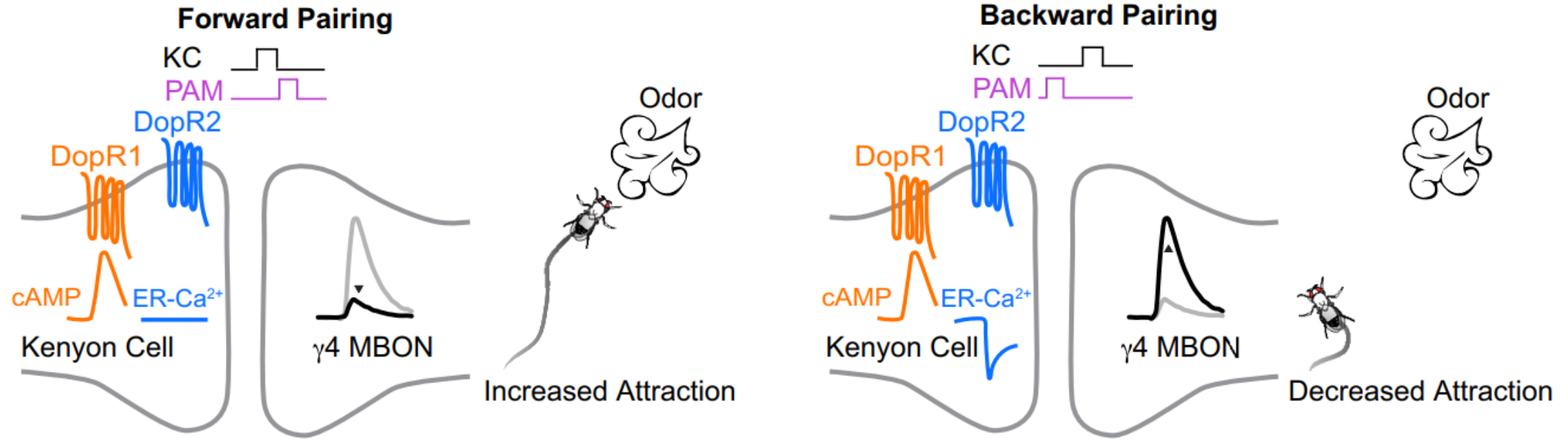


Fig. 9. Cartoon illustrating that forward pairing of an appetitive odor with PAM-DAN stimulation leads to dDA1 receptor activation and cAMP accumulation, a decreased response to the studied MBON, and behavioral attraction. Backwards pairing of the odor and PAM-DAN stimulation leads to DAMB activation and calcium release from the endoplasmic reticulum (ER), an increased response of the MBON, and decreased attraction. Reproduced with permission from [Handler et al. 2019](#).

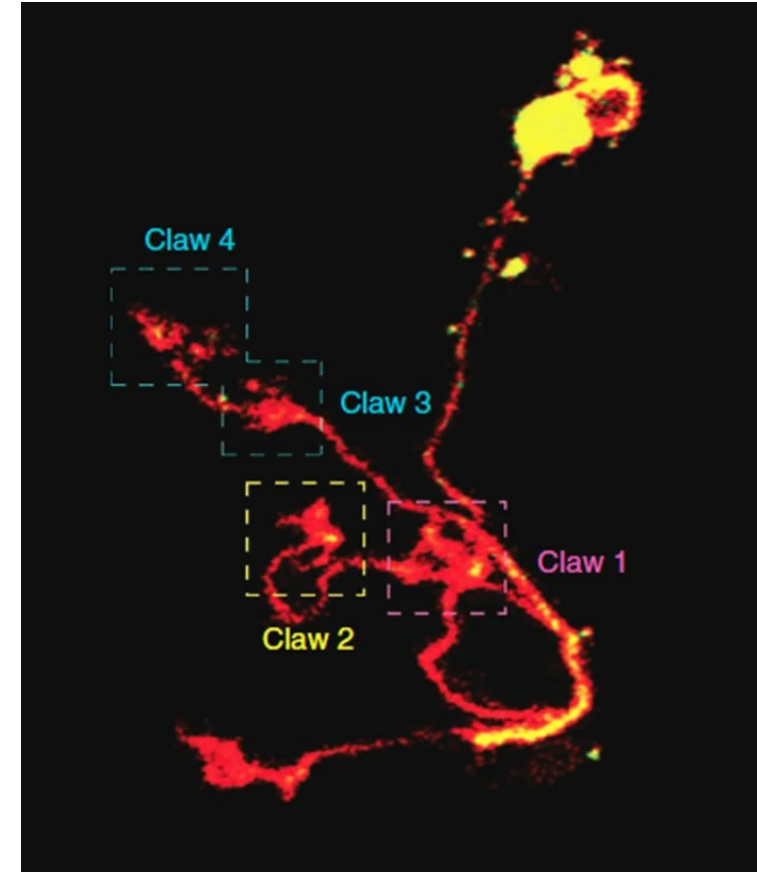
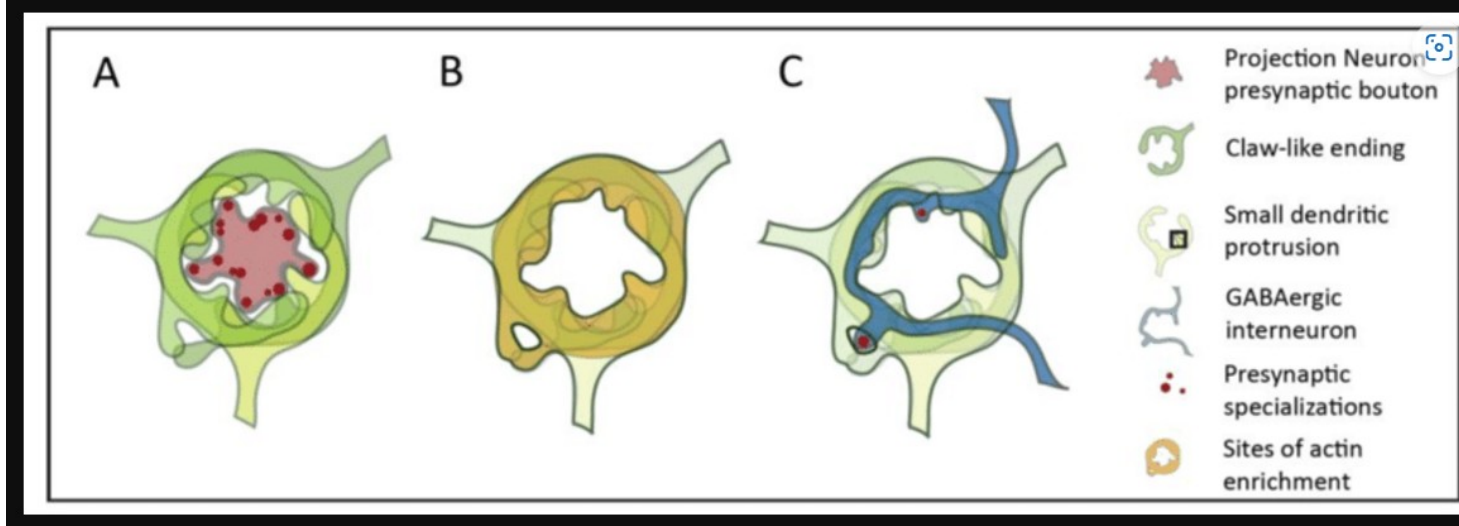
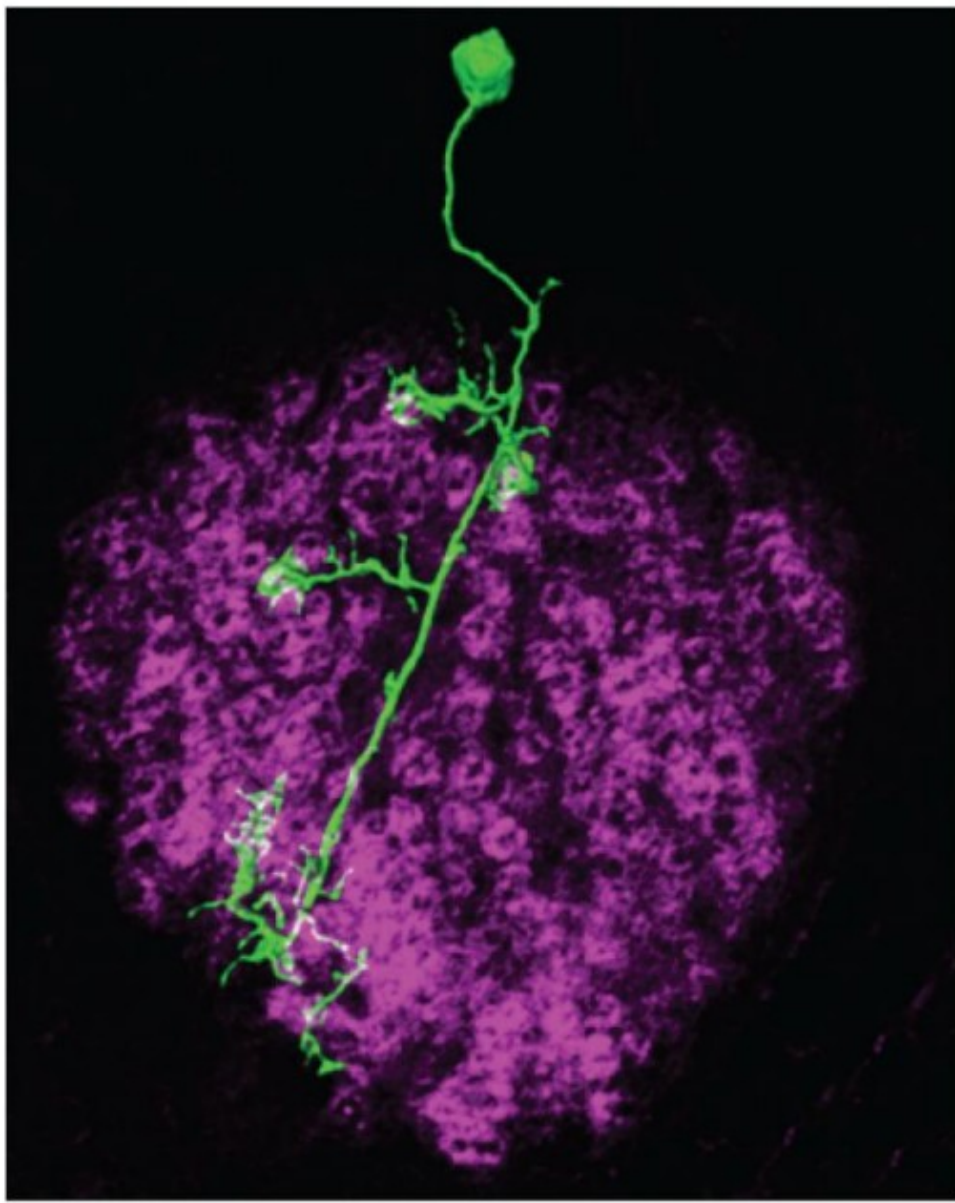


Fig. 10. Dendritic projections from a single MBn (green) extending into the calyx, with claw-like dendritic terminals. The microglomeruli are visible as ring-like structures highlighted by actin staining (magenta). Reproduced with permission from [Leiss et al. 2009](#).

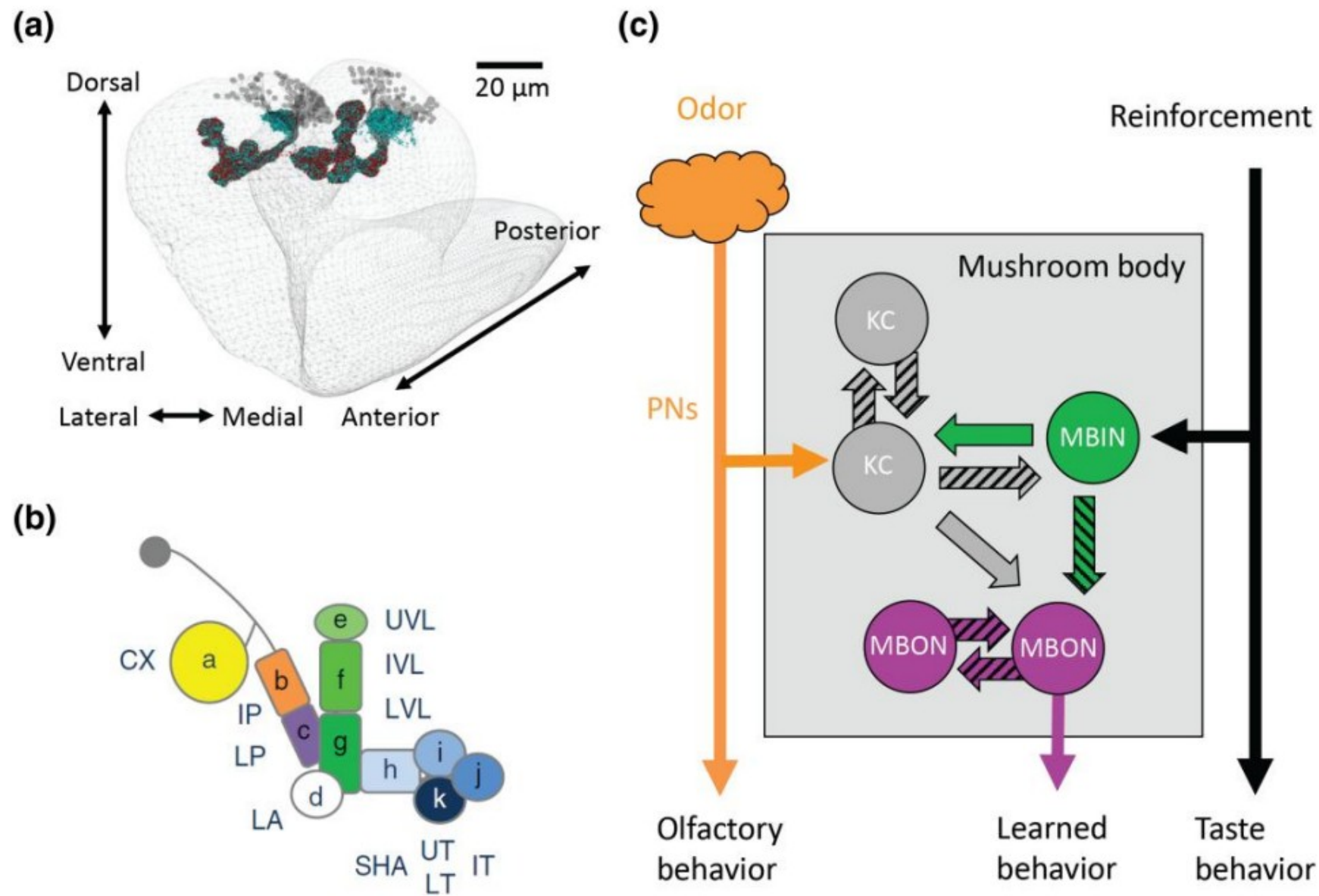


Fig. 11. a) a reconstruction of the larval MB from 3-dimensional electron microscopy, showing the MBn cell bodies, the calyx, and the MB vertical and horizontal lobes. b) The MB lobes have both input neurons (MBn) and output neurons (MBOn), organized as 11 compartments. c) The circuit organization is like adult flies, with Pn providing olfactory input to the MBn, the MBn providing input to both the MBn and MBOn, and with reciprocal communication between the population of MBn and the population of MBOn. Reproduced with permission from [Thum and Gerber 2019](#).

Learning and memory using *Drosophila melanogaster*: a focus on advances made in the fifth decade of research

Ronald L. Davis*

Department of Neuroscience, Herbert Wertheim UF Scripps Institute for Biomedical Innovation & Technology, University of Florida, 130 Scripps Way, Jupiter, FL 33458, USA

*Corresponding author: Email: ronaldldavis@ufl.edu

Abstract

In the last decade, researchers using *Drosophila melanogaster* have made extraordinary progress in uncovering the mysteries underlying learning and memory. This progress has been propelled by the amazing toolkit available that affords combined behavioral, molecular, electrophysiological, and systems neuroscience approaches. The arduous reconstruction of electron microscopic images resulted in a first-generation connectome of the adult and larval brain, revealing complex structural interconnections between memory-related neurons. This serves as substrate for future investigations on these connections and for building complete circuits from sensory cue detection to changes in motor behavior. Mushroom body output neurons (MBO_n) were discovered, which individually forward information from discrete and non-overlapping compartments of the axons of mushroom body neurons (MB_n). These neurons mirror the previously discovered tiling of mushroom body axons by inputs from dopamine neurons and have led to a model that ascribes the valence of the learning event, either appetitive or aversive, to the activity of different populations of dopamine neurons and the balance of MBO_n activity in promoting avoidance or approach behavior. Studies of the calyx, which houses the MB_n dendrites, have revealed a beautiful microglomerular organization and structural changes of synapses that occur with long-term memory (LTM) formation. Larval learning has advanced, positioning it to possibly lead in producing new conceptual insights due to its markedly simpler structure over the adult brain. Advances were made in how cAMP response element-binding protein interacts with protein kinases and other transcription factors to promote the formation of LTM. New insights were made on Orb2, a prion-like protein that forms oligomers to enhance synaptic protein synthesis required for LTM formation. Finally, *Drosophila* research has pioneered our understanding of the mechanisms that mediate permanent and transient active forgetting, an important function of the brain along with acquisition, consolidation, and retrieval. This was catalyzed partly by the identification of memory suppressor genes—genes whose normal function is to limit memory formation.

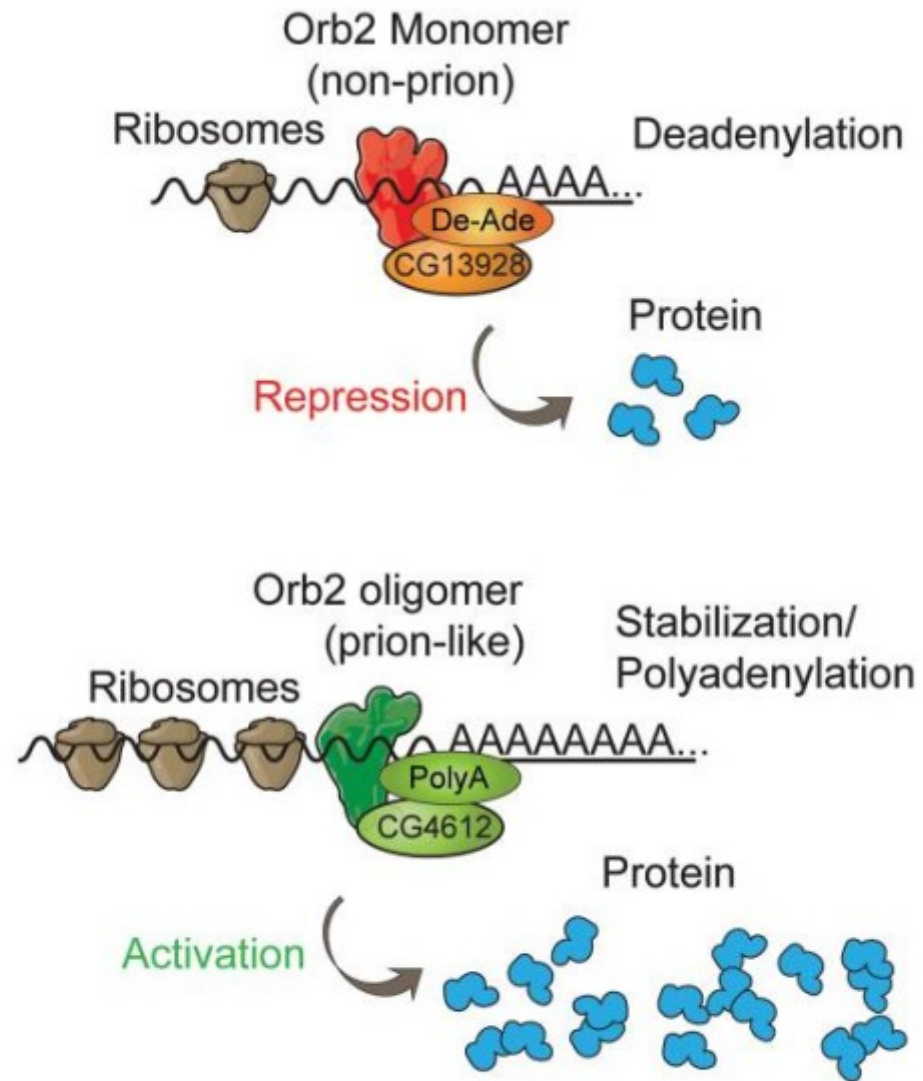


Fig. 12. Model for the role of Orb2 monomers and oligomers in mRNA stability and protein translation. Reproduced with permission from [Khan et al. 2015](#).

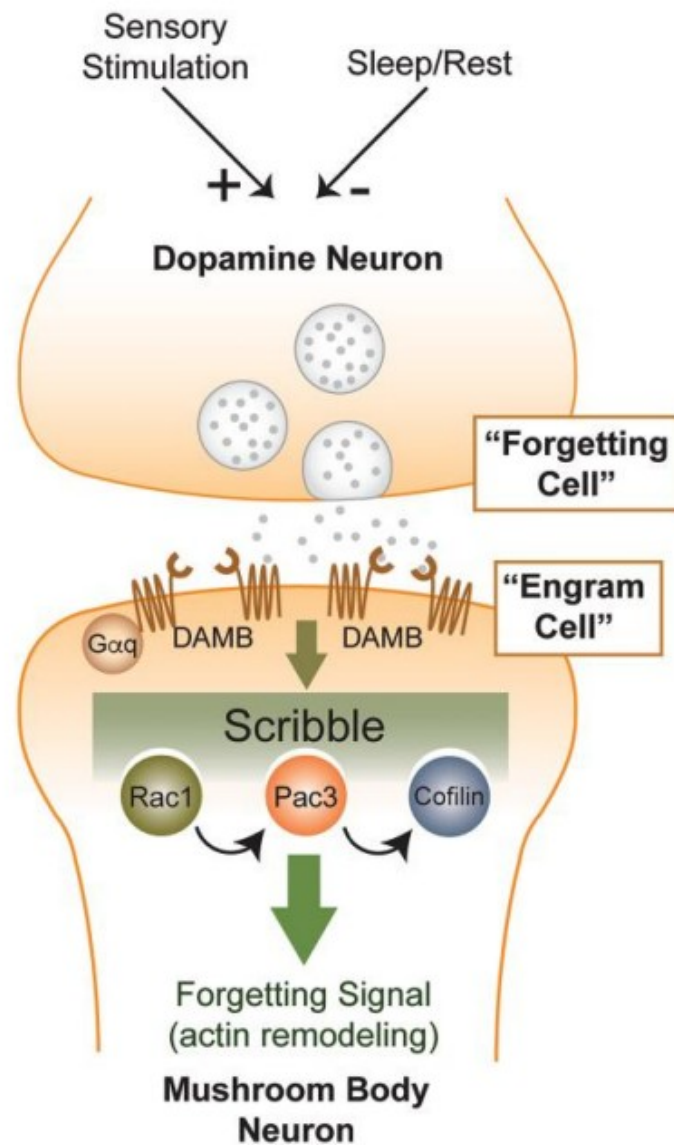


Fig. 15. Model for DA-based forgetting of olfactory memory. In this model, the chronic and slow release of DA is envisioned to slowly degrade memory traces in MBn or other associated neurons, through the DAMB receptor coupled to $G_{\alpha q}$, the Scribble scaffolding complex and $Rac1 \rightarrow Cofilin$ components, and the actin cytoskeleton. Reproduced with permission from [Davis and Zhong 2017](#).

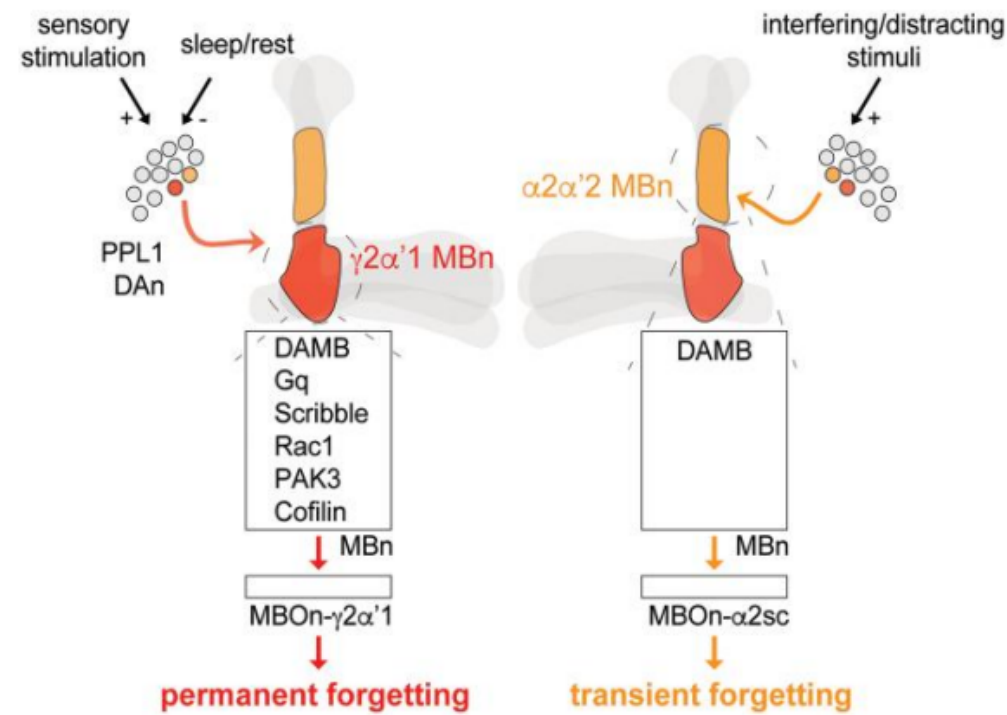


Fig. 16. Model comparing “permanent vs” transient forgetting. Two forms of forgetting include permanent (red) and transient (orange) forgetting. Permanent forgetting involves a PPL1 DAN that synapses onto the $\gamma 2\alpha'1$ -MBn (junction) compartment (red). The slow, ongoing DAN activity after learning is transduced by the G_q-coupled, DAMB receptor. This forgetting signal mobilises the Scribble scaffolding complex and recruits Rac1, PAK3 and Cofilin to erode labile, nonconsolidated memory. The cellular memory traces formed and stored in the following neuron, $\gamma 2\alpha'1$ -MBO_n, are also eroded. This process can be exacerbated by enhanced sensory stimulation, or repressed by sleep/rest (Berry *et al.* 2015). Transient forgetting incorporates a different PPL1 DAN that synapses onto the $\alpha 2\alpha'2$ -MBn compartment (orange). This forgetting signal, transduced by DAMB, temporarily impairs the expression of consolidated, PSD-LTM. A cellular memory trace stored in $\alpha 2sc$ -MBO_n is not abolished after activating the forgetting pathway. This process can be triggered by interfering or distracting stimuli to transiently block the retrieval of PSD-LTM. Reproduced with permission from Sabandal *et al.* 2021.